SKBF
KBS
TEKNISK
RAPPORT
83-10

Radiolysis in nature: Evidence from the Oklo natural reactors

David B Curtis
Alexander J Gancarz

New Mexico, USA February 1983

SVENSK KÄRNBRÄNSLEFÖRSÖRJNING AB / AVDELNING KBS

POSTADRESS: Box 5864, 102 48 Stockholm, Telefon 08-67 95 40

RADIOLYSIS IN NATURE:
Evidence from the Oklo Natural Reactors

David B Curtis
Alexander J Gancarz

New Mexico, USA February 1983

Denna rapport utgör redovisning av ett arbete som utförts på uppdrag av KBS-projektet. Slutsatser och värderingar i rapporten är författarnas och behöver inte nödvändigtvis sammanfalla med uppdragsgivarens.

En förteckning över hittills utkomna rapporter i denna serie under 1981, återfinns i slutet av rapporten. Uppgift om KBS tidigare tekniska rapporter från 1977-1978 (TR 121), 1979 (TR 79-28) och 1980 (TR 80-26) kan erhållas från SKBF/KBS.

RADIOLYSIS IN NATURE:

Evidence from the Oklo Natural Reactors

David B. Curtis

Alexander J. Gancarz

TABLE OF CONTENTS

SUMMARY		i
1.	Introduction	1
2.	GEOLOGIC SETTING	2
	2.1 General	2
	2.2 Layer C-1	2
	2.3 Mineralogy	3
	2.4 Age	5
3.	NUCLEAR REACTOR ZONES	6
	3.1 General	6
	3.2 Reactor Zone Geology	8
	3.3 Operating Temperatures and Pressures	10
4.	MINERALOGY AND GEOCHEMISTRY	12
	4.1 Argillaceous Minerals	12
	4.2 Chemical Rock Types	14
	4.3 Iron Geochemistry	15
	4.4 Uranium Geochemistry	17
	4.5 Plutonium Stability	20
	4.6 Fission Products	21
	4.7 Carbon Geochemistry	22
	4.8 Fluid Phase	22
5.	SIMPLIFIED DOSE CALCULATIONS	24
	5.1 Alpha Particle Dose	24
	5.2 Beta Particle Dose	27
6.	RADIOLYSIS	29
	6.1 Introduction	29
	6.2 Iron	30
	6.3 The Radiation Yield of Hydrogen	33
	6.4 Element Transport From the Reactor Zones	34
7.	COMPARISON WITH THE SWEDISH NUCLEAR FUEL SAFETY PROJECT	40
References		42
Tables		45
Figures		56

SUMMARY

An examination of the mineralogy of the reactor zones at Oklo shows that they have been significantly altered. The rocks immediately adjacent to these zones are also mineralogically modified with respect to normal uranium bearing rocks. There are also significant chemical changes that correlate with the altered mineralogy. Both changes are interpreted to have been attendent upon the operation of the reactors. The mineralogic changes appear to be the consequence of radiation damage, changes in the bulk chemistry of the system and increased temperatures. Chemical changes were the consequence of convectively circulating fluids that transported elements in and out of the rocks. There were also changes in the electrochemical conditions in the rocks. These changes can most reasonably be attributed to oxidizing and reducing species produced by the radiolysis of water.

We have examined the available data to determine the effects of radiolysis products on the rocks. In addition,we have calculated radiation doses and examined the production of radiolysis products in the fluid phase. Quantification and interpretation of these data lead to the following conclusions: 1) There was a net reduction of iron, probably associated with a net increase in total iron in the rocks of the reactor zones. The reduction of iron was most likely the result of hydrogen produced by the radiolysis of water. 2) Commensurate with the iron reduction, there was an oxidation of uranium and multivalent fission products, resulting in their transport out of the reactor zone. Approximately 10% of the uranium and various proportions of these fission

products were removed and redeposited in rocks within a few meters of the reactor zones. 4) The calculated radiation doses from alpha radiation and the inferred hydrogen production suggest an effective radiation yield of 0.06 molecules of hydrogen per 100 eV of energy imparted to the fluid phase. Considering radiation from both alpha and beta sources, the G value for hydrogen production is reduced to 0.01 to 0.002 molecules H_2/100 eV.

1. INTRODUCTION

In 1972, remnants of naturally occurring nuclear fission reactions were discovered in uranium ore bodies in Precambrian sedimentary rocks from Gabon, Africa (1). A map showing the location of Gabon and the Oklo Mine appears in Figure 1. The properties of this natural occurrence were analogous to those of modern power-generating nuclear reactors. The nuclear products have existed in a geologic environment for almost half the age of the earth and, thus, offer the opportunity to investigate what might result from attempts to dispose of commercially generated high-level nuclear waste for long periods of time in geologic repositories. In terms of natural processes, the intense radioactive fluxes associated with these reactors are unique, and as such, the fossils of the nuclear reactors preserve an unprecedented record of the long-term effects of high levels of radioactivity on materials of the earth's crust.

2. GEOLOGIC SETTING

2.1 General

Evidence for the existence of natural reactors was found in a uranium mine in the Franceville Basin, located in the Republic of Gabon in equatorial Africa. The Oklo mine is in the basal section of the Francevillian Series, a sequence of Precambrian,unmetamorphosed volcanic and sedimentary rocks lying uncomformably on the metamorphosed basement of the du Chaillu and North Gabon massifs (2). The Francevillian Series is divided into five major formations, F_A through F_E. The basal section, F_A, is approximately 900 meters thick and consists of fluviatile sandstone, conglomerate, and argillaceous and carbonate cement. Uranium enrichment occurs at the top of F_A in a stratum called C-1. Immediately overlying C-1 is the F_B formation which is composed of variegated and black pelite, dolomite and manganese-rich carbonate (3). Deposition of the Francevillian sediments occurred at some time between 2.1 and 2.7 billion years ago (4).

2.2 Layer C-1

The stratigraphy of the reactor bearing zone, C-1, has been defined in detail (3). It is underlain by a 5 to 20 centimeter thick layer of quartz-pebble conglomerate which forms the west wall of the Oklo quarry. Immediately overlying the conglomerate are sedimentary sequences identified as C-1 (a-b). These strata, called the "fine sandstones of the wall", are 0.8 to 1.5 meters thick and very uniform on the scale of the deposits. C-1a is

often pelitic and may be green or black in color, whereas C-1b is always a black sandstone, usually fine-grained but with occasional lentils of medium-grained sandstone. Sometimes a 5 to 10 centimeter thick conglomerate will separate C-1a from C-1b. Strata C-1 (c, d, e) are medium- to fine-grained sandstone with an overall thickness of about one meter. C-1 (f, g, h, i) each begins with a conglomerate and grades upwards to a coarse- or medium-grained sandstone at the top. Occasionally, less than 10 centimeters of fine-grained sandstone are at the top of these strata. These fine-grained, basal conglomeratic units are very persistent throughout the mine and are used as reference data. The sequence is covered with pelite which marks the base of the overlying F_B formation. Pelitic rocks of F_B are cut by a channel of sandstone, the core of which is located in the northern part of the quarry.

2.3 Mineralogy

The pelitic sandstone of C-1 contains a fine-grained, phyllite matrix. Occasionally, there are altered remnants of large biotite crystals and silt-sized particles of detrital quartz, all oriented parallel to the bedding plane. Except for material around the fossil reactors, the only argillaceous minerals are illite and chlorite. Generally illite is more abundant than chlorite in the pelitic seams. In contrast, chlorite is more abundant than illite in the phyllite cement of the sandstone and conglomerate (5). Illite in the sediments is predominantly a polymorphous variety, 1Md. There are small quantities of the $2M_1$ polytype that are attributed to a detrital source. The more

abundant 1Md illite is generally characteristic of minerals crystallized in deep diagenesis (5).

In the mineralized strata, the average uranium concentration is about 0.2%. There are, however, small pockets with dimensions tens of centimeters to a meter thick, where the uranium is much more concentrated. In these pockets the uranium content ranges up to and in excess of 60%. Petrographic and field studies have shown that the very rich zones are the result of a secondary uranium mineralization. The strata have been upturned and gently folded; associated with the deformation are faults and fractures. This deformation occurred subsequent to the first mineralization, as demonstrated by the observation that these fractures cut across detrital quartz grains surrounded by uraninite and encased in secondary quartz cement. The secondary uranium minerals are deposited along the fracture planes (3).

Uranium minerals outside the reactor zone are predominantly pitchblende, the massive, colloform oxide of tetravalent uranium. The silicate of reduced uranium, coffinite, is observed less frequently in these ores and may be the result of alterations which postdate the reactor operation. A nondescript mineral of oxidized uranium referred to as "gummite" is seen in the ores, but it is always considered to be a product of late stage alteration (5).

Uraniferous ore that has not been involved in the nuclear reactions is generally of two types. The most common type contains

contains between 0.2% and 0.5% uranium as pitchblende in association with disseminated carbonaceous material. This material is often oxidized (6) and contains globules of polymerized asphalt (7). Abundances of organic carbon in a variety of rock types at Oklo are given in Table 1. This first type is a uraniferous sandstone composed of recrystallized quartz with chlorite and illite in various proportions. Sulfides of lead and iron are abundant. A second ore type is a slightly silicified,black sandstone containing 5% to 25% UO_2 as pitchblende. Carbonaceous substances are rare in this type of mineralized rock. Pitchblende is distributed around, but never in direct contact with hematite. The two are never in direct contact, but separated by a border of colorless material. This arrangement suggests "small oxioreduction front on a scale of 10 cm" (3). These ores are associated with zones of tectonic activity. Uranium minerals cover the surfaces of microfractures in quartz and sandstone.

2.4 Age

The uranium and lead isotopic abundances in the ores show that they formed $2.05 \pm .05 \times 10^9$ years ago (8, 9, 10). Analyses of rubidium and strontium isotopic composition indicate that the sediments were diagenetically altered at times up to 1.8×10^9 years ago (4). Interpretation of the lead isotopic data suggests that lead has been more or less continuously lost from these rocks throughout their entire geologic history (10). This is an important observation since it suggests the presence of a mobile phase throughout the geologic history of the ore-bearing rocks.

3. NUCLEAR REACTOR ZONES

3.1 General

Extreme uranium enrichment, combined with other unique characteristics, produced circumstances that allowed sustained periods of nuclear fission in small volumes of rock within the mineralized stratum now being mined at Oklo. Conditions for sustained criticality included the following: 1) low abundances of elements with large neutron cross sections that would "poison" the nuclear reactors, 2) enough hydrogen (presumably in the form of water) to moderate neutrons from the fissioning 235-uranium, 3) appropriate enrichment of uranium in an acceptable geometric arrangement to sustain nuclear fission, and 4) enrichment of 235-uranium relative to 238-uranium compared to that found in "normal" uranium today. The latter criterion was met in the past because of the differences in the decay rates of the uranium isotopes. Two billion years ago, 235-uranium constituted nearly 4% of the isotopes of natural uranium.

The time of reactor criticality inferred from isotopic analyses of the uranium fuel and the fission product neodymium, is consistent with ranges from 1.6 to 2.0 billion years (11) and 1.93 to 2.5 billion years before the present (12). It seems reasonable to assume that the time of criticality was soon after the time of uranium mineralization. The more precisely defined time of this latter event, 2.05 billion years ago, has been used as the time of reactor criticality in recent work (13). Studies of the reactor

operating parameters limit the duration of reactor criticality to periods of time between one and five hundred thousand years (11, 13).

As of 1978, four distinct sites of sustained nuclear fission had been identified at the Oklo mine. The total uranium involved in the nuclear reactions was estimated to be 8×10^5 kilograms, corresponding to 6×10^3 kilograms of fissioned 235-uranium. At the present, 13 reactor zones have been discovered, and the estimate of fissioned 235-uranium has been increased to approximately 1.2×10^4 kilograms. Of the 4×10^3 kilograms of the 239-plutonium that were produced, some small fraction (0 to 10%) fissioned or underwent neutron capture. The majority decayed to 235-uranium. This is important since, as will be discussed in a subsequent section, the decaying 239-plutonium is the predominant source of alpha particles producing radiolytic effects in the surrounding aqueous fluid.

The isotopic composition and relative abundances of uranium and neodymium can be used to calculate the neutronic characteristics of the reactors. Curtis, et al., (13) determined that the thermal plus resonance neutron fluences were as high as $10^{21} n/cm^2$. Furthermore, they concluded that decaying fission products produced approximately 10^{28} beta-gamma emitting disintegrations during the reactors' lifetime. The total energy production at the Oklo reactors is estimated to have been 1.65×10^4 MW-years. The duration of the reactor criticality was a few hundred thousand years. This corresponds to an average thermal loading within the reactor zones

of about 50 W/m^2. There is some variation from zone to zone. Using a factor of 1 MW-day/gram of 235-uranium fissioned, an energy output of 1.5×10^4 MW-years was estimated for zone 2, corresponding to a thermal loading of 140 W/m^2. In contrast, in zones 3 and 4 the energy output was only 1.5×10^3 MW-years with a correspondingly lower thermal loading of 5 W/m^2.

3.2 Reactor Zone Geology

Rocks that contain the remnants of the nuclear reactors and those that immediately surround them are anomalous compared to the rest of C-1. In this sandstone environment, the reactor zone rocks exhibit few sedimentary features. The zones can be generally characterized as a reactor core, where the sustained nuclear reactions actually occurred, and a series of aureoles extending for a distance of about two meters from the site of reactions.

Weber (14) in his synthesis of geologic studies of the nuclear reactors makes the following statement.

> "For a long time it was thought that the peculiarity of the ore from the natural reactors was due to exceptional conditions of placement of the uranium, which would explain its high content. The disappearance of the sandstone horizons from the mineralized stratum C-1 was time and again attributed to local sedimentological variations, and to tectonic 'compression'. The thought was that the discovery of an ore with an argillaceous gangue beyond the reaction zones would make it possible to determine certain characteristics of this ore that had been modified by nuclear reactions. However, while ores with an argillaceous gangue whose isotope content was practically normal were encountered on occasions, they were always at the border of the reaction zones...,and they could in no way be considered as evidence of 'normal' argillaceous ores completely spared by nuclear reactions. Little by little it was realized

> that this rich ore with an argillaceous gangue did not exist beyond the reaction zones and their perimeter of influence, that this ore had attained its present state as a result of the nuclear reactions from normal sandstone."

Although there are aspects of this perspective that have not been satisfactorily explained, it seems that the reaction zones and their "perimeter of influence" are direct manifestations of changes in the physical and chemical environment induced by the nuclear reactions.

Zones of criticality occur as separate and distinct features in the mineralized strata, each clearly separated from the other. A zone comprises a relatively small volume of rock on the order of a few hundred cubic meters. Each feature is thin, less than one meter thick, in the dimension perpendicular to the stratigraphic plane and extends for 10 to 20 meters along the dip of the mineralized stratum. The reactors extend along a north-south line in the plane of C-1. The most northerly (zone 1) is the nearest to the surface and each is located deeper as they occur to the south. Reactor zone 2 has been studied most thoroughly. More than a thousand samples were collected from zone 2, and a large fraction of them have been analyzed for their mineralogic, petrographic, isotopic and chemical properties. Zones 1, 3-4, 5-6, and 9 have been studied to a lesser degree. Zone 2 sustained the most intense nuclear activity. The fissions per gram of rock, neutron fluences and 235-uranium deficiencies are significantly greater in zone 2 than in any other. Most of the

conclusions in this paper are based upon observations from this zone.

3.3 Operating Temperatures and Pressures

Estimates of temperature and pressure during the period of criticality have been made. Three independent temperature estimates have been made. Vidale (15) examined the mineral assemblages and concluded from the assemblage, biotite plus muscovite, that the temperatures must have been in excess of 400°C in the reactor, and that 400°C temperatures could have extended for ~4 meters from the edges of the zones. Neutron capture by 175-lutetium and 155-gadolinium are temperature sensitive, since the resonance neutron capture cross-sections are Doppler broadened with temperature. Studies of the lutetium and gadolinium isotopes suggest temperatures in the range of 280°C to 400°C (16). Inclusions in mineral grains which formed during the period of nuclear fission contain aqueous fluids. Studies of the inclusions indicate that the fluids were heated to temperatures between 450°C and 600°C (17).

Based on the polymorphism of the illite, the temperatures around the reactors during their operation have also been estimated. The transformation of illite from 1Md to $2M_1$ occurs at approximately 250°C. The normal sediments of the F_A formation contain 1Md illite, but in an aureole about 1.5 meters thick around the reactors $2M_1$ illite occurs, suggesting that the temperatures were in excess of 250°C. In the reactor zones themselves 1M illite occurs. It is reasoned that the original mineral lattices

were destroyed due to the intense radiation doses and recrystallized after the reactors ceased operation (18) and the temperatures were reduced: hence 1M illite. The ambient temperature estimated from the depth of burial must have been approximately 130°C.

In summary, it seems reasonable that the reactors operated in the temperature regime of 400°C to 600°C and that the thermal effects extended outward at lower temperatures to a few meters. Curtis, et al., (13) investigated the transport of fission product ruthenium and technetium and concluded that they were transported in part during a few hundred thousand year "thermal" period after the reactors ceased operating and must have been transported in the temperature regime of 100°C to 425°C.

Fluid inclusions were also used to determine the pressure in the rocks at the time of nuclear criticality (17). It was concluded from examining inclusions formed during the operation of the reactor that pressures were between 800 and 1070 bars.

4. MINERALOGY AND GEOCHEMISTRY

4.1 Argillaceous Minerals

Mineralogic changes in both reactor zones and their zone of influence reflect chemical and physical conditions associated with the operation of the reactors. The gangue of the ore within these two zones is characterized by the complete or partial loss of quartz. This is in marked contrast to the surrounding sandstone where quartz is a major mineral. Dissolution of quartz is attributed to its increased solubility in hot aqueous fluids (14). Dissolved silicon dioxide was transported away by convectively driven hydrothermal fluids, leaving a residue consisting of the less soluble argillaceous minerals (3). This phyllitic residue itself was altered by the chemical and physical environment attendant with the operation of the reactors and resulted in a mineral assemblage unique to the Francevillian Series.

Aureoles around the reactor zone are defined primarily by the mineralogy of the phyllite (19). The outer aureole is characterized by a deficiency of the 1Md polymorph of illite, the variety most commonly found in the surrounding sediments, and an enrichment of the $2M_1$ polymorph. In cases where the enclosing rocks are sandstone, (zones 3-4 and 5-6), this outer aureole contains quartz crystals that microscopically show signs of desilicification. If the encompassing rocks are pelitic (zones 1 and 2), the $2M_1$ illite aureole is lacking quartz. The demarcation between this zone and normal sediments usually occurs about 1.5 meters

from the reaction zone. The $2M_1$ illite is a high temperature polymorph. It is thought that the deficiency of 1Md and excess of the $2M_1$ variety reflect a transformation in response to the higher temperatures produced by the nuclear reactions. At a distance of about 70 centimeters from the reactor zone there is a sharp transition distinguishing the outer aureole from the inner aureole. Chlorite replaces illite as the dominant phyllosilicate and quartz is never found in the rocks. Compared to chlorite in normal sediments, that in this zone is magnesium-rich.

Within the reactor zone quartz has been completely removed and illite is again the predominant phyllitic mineral. It is the 1M polymorphous type and differs from that found in the rest of the rock of C-1 in that it contains sodium, and has smaller concentrations of potassium and greater abundances of iron and magnesium. Chlorite in the gangue of the reactor zone contains a greater proportion of iron relative to magnesium than chlorite in the adjacent aureole. The chlorite is often in various stages of alteration to vermiculite. It is paradoxical that illite in the aureole reflects increased temperatures while that in the reactor zone, where it must have been hotter, reflects lower temperatures. Based upon the lack of radiation damage in the argillaceous minerals of the gangue, it has been proposed that this 1M illite formed from "radiation-produced aluminosilicate mud at temperatures less than the maximum attained during criticality" (18).

4.2 Chemical Rock Types

We used the chemical data of Branche et al. (20) and normalized all element abundances to aluminum. This element is believed to be conservative and therefore aluminum normalized abundances can be directly compared in rocks with extremely variable densities. These normalized results are presented in Table 2. In doing so, we identify types of rocks in and around reactor zone 2 that bear distinct chemical characteristics. While we cannot specifically associate these chemical types with the mineralogically well-defined aureoles, there is probably a close correlation between the unique compositions and the mineralogy of the rocks. Type 1 consists of rocks that clearly sustained nuclear fission. They have a high uranium content and are distinguished by high U/Al (5.1 to 44), K/Al (0.07 to 0.19) and Ca/Al (0.09 to 0.81) values. They also show marked depletion of 235-uranium relative to 238-uranium although this was not a criterion for defining them. Type 2 rocks differ from type 1 in that they have smaller U/Al (1.0 to 3.5) and Ca/Al (0.03 to 0.10) ratios. These rocks are not universally characterized by large deficiencies of 235-uranium relative to 238-uranium characteristic of samples from the heart of the reactor cores. A large group of samples of this type from the 2N traverse contain $^{235}U/^{238}U$ values only slightly lower than normal. Chemical types 3 and 4 appear to be from outside the reactor zone. They both have small U/Al (0.0007 to 0.15 and 0.14 to 0.38) and Ca/Al (0.003 to 0.05 and 0.02 to 0.03) values. Chemical type 3 is

distinguished by large Mg/Al (0.61 to 1.4) and small K/Al (0.002 to 0.09) values, properties consistent with the magnesian chlorite rocks of the inner aureole. While type 4 has a fairly high K/Al (0.10 to 0.36) it is also unique in that it has large Si/Al (2.0 to 4.7) in contrast to all other types that have Si/Al values from 0.83 to 2.1. These rocks cannot be obviously identified as one of the mineralogically defined aureoles. The composition that distinguish each of the chemical rock types are included in Table 2 and the samples are classified according to chemical type. Those that do not fit the defined criteria have not been classified.

4.3 Iron Geochemistry

Except for uranium, iron is the most abundant multivalent element in these rocks. Consequently, its chemistry and mineralogy are likely to be important indicators of changes in electrochemical conditions produced by the radiolysis of water. Hematite (Fe_2O_3) is the most abundant non-silicate mineral of iron. It occurs in the reactor zone, but is absent from the aureoles (19). Hematite is occasionally observed as pseudomorphs of pyrite (7) and in fluids incorporated into quartz crystals at the time of nuclear criticality (17). In the reactor zone, hematite commonly occurs as globular or elongated fibrous networks at the center of nodules devoid of uraninite. The ferric oxide is surrounded by a light colored mineral lacking in both hematite and uraninite (19). Ferrous iron oxides are apparently totally absent.

Probably the most abundant non-silicate mineral of ferrous iron is pyrite, although this sulfide is a rare constituent of the reactor zone (7). Mineralogic descriptions of eighteen samples from the heart of the reactor zone contain no mention of pyrite. Pyrite occurs sparsely as veinlets and euhedral grains of this mineral are observed in association with veins of carbonaceous matter cutting across the reactor zone (21).

The majority of iron in these rocks is included in phyllosilicate minerals. Virtually all the ferrous iron is included in illite and chlorite, while oxidized iron is included in both argillaceous minerals and hematite (20). Uraninite contains about 0.5% iron in an unspecified but presumably reduced state (21).

There has been a preferential reduction of iron in the reactor zones, probably associated with a net gain of the element. Table 3 presents the data on iron in reactor zone 2. These data are plotted in Figure 2. Normal rocks of C-1 typically have Fe^{+3}/Fe^{+2} values of 0.9 and the altered rocks almost always have lower values. While the different chemical rock types exhibit some overlap in this diagram, chemical type 1 rocks (i.e. those that are unambiguously from the reactor zone) plot principally that region of the diagram suggesting that relative to "normal" C-1 rocks, they have a net gain of ferrous iron. Chemical type 2 scatter in the diagram. In contrast, type 3 and 4 rocks, those that we believe were not included directly in the reactor

zone, contain a greater proportion of oxidized iron and tend to plot toward the region of the diagram occupied by C-1 host rocks.

4.4 Uranium Geochemistry

In the reactor zones uranium is found exclusively as the mineral uraninite, a well-crystallized variety of the tetravalent oxide. The abundances are typically 25% to 60% UO_2. Immediately adjacent to the regions of criticality, the uranium mineralogy is an "intermediate type" containing intimate mixtures of uraninite and pitchblende (5, 7). These rocks that are transitional from the reactor zones to "normal" ores also contain coffinite, the silicate of tetravalent uranium.

Uraninite is absent outside the reactor zones and their immediate surroundings. It represents a temperature-induced transition of pitchblende, the predominant uranium mineral in "normal" Oklo ores. Uraninite shows a remarkable stability in rocks of the reactor zones despite high temperatures, intense radiation fluxes and convecting aqueous fluids. Evidence for the physical stability of this mineral is found in the high concentrations of incompatible fission products in individual uraninite grains (22). In addition, the mineral grains still contain radiation damage incurred during nuclear criticality (18).

The chemical stability of uraninite in the reactor zones is obvious from isotopic studies. Multiple reactor operating parameters can be reconstructed from the isotopic composition of uranium and rare earth fission products (principally neodymium) in hand-sized specimens from the reactor zones (11, 13, 23, 24, 25). There is a remarkable consistency in these parameters from sample to sample from the same reactor zone.

In the reactor zones 235-uranium was destroyed by fission and created by the decay of 239-plutonium which was produced by neutron capture of 238-uranium. Consequently the ratio $^{235}U/^{238}U$ varies from sample to sample according to a number of parameters, such as neutron flux, the neutron energy spectrum, and the absolute concentration of uranium. All samples that have been measured at Oklo contain uranium that has either normal isotopic composition (^{235}U = 0.72 atom %) or is depleted in 235-uranium. The lowest 235-uranium isotopic abundance is on the order of 0.3 atom % 235-uranium; typically in zone 2 this value is 0.5 to 0.6 atom %. However, there is homogeneity of the uranium isotopic composition on a scale that is expected from the mean free path of neutrons in the rocks. Different portions of a few centimeter-sized hand specimens contain uranium with the same isotopic composition. Uraninite and clay from the same sample are isotopically homogeneous with respect to uranium (25). Even single uraninite grains do not show variations of uranium isotopic composition from core to rim (26). This homogeneity strongly suggests that ura-

nium was not significantly mixed from one region of the reactor zone to another, and that normal uranium was not transported from the surrounding rocks and deposited in the reactor zones. In the words of Naudet (25), "Thus we can very strongly conclude that there is not a significant remobilization of uranium in the core, i.e., that the uranium found there was there at the time of the reactions, that it has not been displaced and that there has not been any significant input after the start of the reactions."

Despite the apparent stability of uranium within the reactor zones, Naudet (25) states, "It cannot be excluded that a little uranium has been definitely eliminated from the reaction zone by solubilization." It is difficult to distinguish whether the depletion of 235-uranium in rocks adjacent to the reactors were due to "leakage" neutrons or if 235-uranium depleted uranium were transported and deposited into the peripheral rocks. However, Naudet (25) discusses the presence of such isotopically perturbed uranium in the "walls" and "lateral edges" of the reactor zones and concludes that it represents small quantities of uranium transported from the reactor zone. The deposition of this uranium does not extend to distances beyond 2 meters of the zone. At distances greater than this the occurrence of 235-uranium depletion is extremely rare. This mobilization of uranium appears to have occurred on a scale similar to that defined by the mineralogically altered aureoles.

Table 4 contains the characteristics of uranium in samples whose

major element data are in Tables 2 and 3. Chemical type 1 contains uranium that has large deficiencies of 235-uranium. As we stated before, this chemical rock type is clearly from the heart of the critical zones. In contrast, types 3 and 4 contain uranium that is only slightly deficient in 235-uranium compared to normal. It is likely that these deficiencies do not reflect the effects of fission produced in-situ. Instead,they probably contain small quantities of 235-uranium depleted uranium transported from the reactor zone. Samples classed as chemical type 2 are ambiguous. Some of them are very deficient in 235-uranium; these certainly sustained criticality. However, other type 2 rocks contain large quantities of uranium with very small depletions of 235-uranium. It is not certain whether these did indeed support low levels of nuclear fission and the 235-uranium was generated in-situ or whether they contain 235-uranium depleted uranium transported from another region.

4.5 Plutonium Stability

The isotopic evidence for the stability of uranium also provides evidence for the stability of plutonium. Fractionation between plutonium and uranium during the few hundred thousand years the 239-plutonium existed in the reactors would produce local inconsistencies in the nuclear operating parameters, inhomogeneities of the uranium isotopic composition if the fractionation were on a small scale, and enrichment in 235-uranium relative to normal uranium if plutonium were preferentially transported away from the zones of reactions. None of these properties have been observed.

4.6 Fission Products

The Oklo reactor fossils are unique in geology in that aspects of their chemical stability can be assessed by isotopic analyses of the rocks. Isotopic abundances of nuclear products measured by isotope dilution mass spectrometry can be used in conjunction with models of the operating history of the core to reconstruct the composition of these rocks with respect to about thirty elements that were produced and destroyed by the nuclear processes (11, 13, 24, 27). Comparisons between the quantities of nuclear products produced in the rocks and the measured abundances in them now provide a quantitative measure of loss or gain of elements in the reactor zones. Such studies show that fission-produced rare gases, halogens, alkali and alkaline earth elements have been almost totally removed from the rocks (28). About 80% of the molybdenum, 35% of the 99-technetium, 25% of the ruthenium and small quantities of rare earth elements are missing from the rock. The unique isotopic composition of the nuclear products provides a means of tracing their movement into the surrounding rocks. Studies of ruthenium, 99-technetium and molybdenum indicate that these elements have been transported over distances no greater than 10 to 15 meters (13). In one instance these three elements form a distinct aureole extending about 2 meters from the reactor zone (29). Limits on the time of element transport can be established from the half life of 99-technetium. These temporal limits constrain the time of element movement to the period of reactor criticality and a few hundred thousand years thereafter.

4.7 Carbon Geochemistry

There are limited data on carbon geochemistry. Several workers have suggested that carbon is depleted in the reactor zones compared to that in other uranium rich zones of C-1. The data reported by Vandenbroucke, et al. (6), shown in Table 1, do not convincingly corroborate this suggestion. However, Vandenbroucke, et al. (6) do note an increase in the proportion of oxidized carbon upon nearing the reactor zone. They attribute this to high temperature fluids in and near the reactor zones.

4.8 Fluid Phase

There was convective flow of hot aqueous fluids through the reactor zones during criticality and probably in the time period required for their return to ambient temperature. The existence of aqueous fluids is inferred from several independent sources. One is the necessity to moderate fission neutrons to sustain nuclear criticality. Hydrogen in the form of water is the most likely element to have been the neutron moderator. In addition, a mobile phase was required to effect the chemical changes observed in the reactor cores.

Perhaps the most convincing data are those from the fluid inclusion studies of Openshaw, et al. (17). Certain inclusions are interpreted to be actual samples of the fluid that was circulating through the rocks at the time of nuclear criticality. Sodium normalized abundances of calcium, potassium and magnesium and sulfate/chloride ratios for these fluids are presented in Table 5. Included in

the table are compositions for fluids believed to have been in the C-1 strata at the time of criticality, but not associated with the rocks that sustained the nuclear reactions.

In general, the salinity of both types is similar. The reactor zone fluids are variable in composition. However, in contrast to the normal fluids of C-1, they are enriched in potassium, calcium and magnesium relative to sodium and contain relatively more sulfate than chloride. There was apparently little CO_2 in the fluids; sulfate and chloride appear to have been the only signficant anions (17).

5. SIMPLIFIED DOSE CALCULATIONS

5.1 Alpha Particle Dose

In calculating the dose of alpha particles to be used in the radiolysis model, 239-plutonium was considered first. During the course of the critical period 2500 grams of 239-plutonium were produced per ton of uranium fuel. Since this constitutes only a small fraction of the 238-uranium, we assume a constant plutonium production rate. This is also necessary since no data are available about the time variation of the neutron flux.

The results are shown in Figure 3. The 239-plutonium concentration reaches an equilibrium concentration of 290 grams ^{239}Pu/ton fuel after the first 100,000 years and corresponds to an annual production and decay rate of 0.00833 grams ^{239}Pu/ton fuel/year (3.49×10^{-5} moles ^{239}Pu/ton fuel/year). 90 to 99% of the plutonium decays by alpha decay and the rest fissions or undergoes neutron capture. This is because of the low neutron flux. In considering the contribution of alpha particles we adopt the 95% value.

The other potential plutonium alpha contributors are 238-plutonium and 240-plutonium. Their annual production and decay rates will also reach equilibrium values and are calculated by assuming 5% of the 239-plutonium undergoes neutron reactions and scale by the (n, 2n) and (n, γ) cross sections relative to the total neutron cross section. Hence, 238-plutonium should decay at the rate of less than 4×10^{-10} moles ^{238}Pu/ton fuel/year, and 240-plutonium at the rate of 4.88×10^{-7} moles ^{240}Pu/ton fuel/year. The first is negligible,

the latter contributes less than 2% and will be neglected.

The other element which may contribute to the alpha particle dose is uranium. At 2.05 billion years ago the uranium fuel was 3.82 atom % ^{235}U, hence, 1.60×10^{-7} moles ^{235}U/ton fuel decay per year. This is small relative to the 239-plutonium and less than a 3% contribution even if the equilibrium quantity of daughter products is considered. The decay of 238-uranium is 6.27×10^{-7} moles ^{238}U/ton fuel/year, contributing 1.8% of the alphas of the plutonium. Eight times this many alpha particles will be emitted by the decaying daughters in equilibrium, thereby contributing 14% compared to plutonium, but will not be considered in the total alpha dose.

The range of the alpha in uraninite is 8.91 mg/cm^2 or 8.91 microns for a density of 10 g/cm^2. In water this is 33.2 microns.

The residual range and energy relationships of the 5.155 MeV alpha emitted as 239-plutonium decays were calculated iteratively from range energy relationships in air and the formula (1)

Eq 1

$$\frac{1}{R^r_{UO_2}} = \frac{W_U}{R^r_a \left(0.90 + 0.0275Z + (0.06 - 0.0086Z) \times \log (E^r_\alpha / M_\alpha) \right) - 0.10 Z_U / Z_\alpha} + \frac{W_O}{R^r_a \left(1.00 + (0.06 - 0.688) \times \log (E^r_\alpha / 4) \right)}$$

where W_U = the weight percent uranium in uraninite

W_O = the weight percent oxygen in uraninite

$R^r_{UO_2}$ = the residual range in uraninite of the alpha of energy E

R^r_a = the residual range in air of the alpha of energy E

The relation between E^r and $R^r_{UO_2}$ is shown in Figure 4. E^r is the amount of energy which the alpha from 239-plutonium decay has left after it has traveled some distance through uraninite and can still travel a distance defined by the residual range. This permits us to calculate how much energy can be imparted to a surrounding fluid when the alpha particle escapes from the uraninite. To a reasonable approximation the relationship shown in Figure 4 is linear, and we used a linear formulation in the rest of the calculation.

The next step is to calculate the amount of energy which an average alpha particle produced at some distance from the surface of a uraninite grain will have as it leaves the grain. This can not simply be read from the residual energy and residual range relation, because the alpha particles are emitted isotropically and do not necessarily travel in a normal direction towards the surface of the grain. The average energy of an alpha emanating from a depth is shown in Figure 5. This is a slight underestimation since the curvature of the grain surface was not included. The average energy of the alphas escaping from the grain is 3.52 MeV.

The energy imparted by escaping alpha particles is now simply calculated knowing the average energy, the plutonium concentration

and assuming the grain size. Plotted in Figures 6 and 7 as functions of time are the dose rates (eV/sec/ton fuel) and the integrated doses (eV/ton fuel) for 250 and 500 micron grains.

5.2 Beta Particle Dose

There are two primary sources of beta particles; one is the decay of fission products and the other the decay of 239-uranium (i.e., $^{238}U\ (n, \gamma)\ ^{239}U \xrightarrow[1.2\ MeV]{\beta^-} {}^{239}Np \xrightarrow[0.3\ MeV]{\beta^-} {}^{239}Pu$). Approximately 1 MeV of beta particle energy is released per 235-uranium fissioned and 1.5 MeV for each decay of 239-uranium. During reactor operation 7500 g of 235-uranium fissioned and 2500 g of 239-plutonium were formed per ton of fuel producing a total of 2.9×10^{25} MeV of total energy from beta decay. This is comparable to the 3.1×10^{25} MeV of energy produced by alpha particles from the decay of 239-plutonium.

Beta particles with energies between a few tenths and one MeV have ranges between 100 and 500 microns in contrast to the 8.9 micron range of alphas from 239-plutonium decay. If the radionuclides are included in spherical grains with diameters between 250 and 500 microns, the range differences are such that 10 to 50 times more energy will be released from the host phase by beta decay than by alpha decay. However, if the grains are surrounded by a film of water a few tens of microns thick, the beta particle ranges are large compared to the thickness of the water and we assume only half of the available beta decay energy will be absorbed in water, and the remainder deposited in adjoining minerals. Hence, we estimate with comparable amounts of total energy released by the

two processes, the beta dose to water will be 5 to 25 times that of the alpha dose.

6. RADIOLYSIS

6.1 Introduction

Neretnieks (30) proposed that alpha radiation from nuclear wastes might cause the radiolysis of H_2O,forming reducing species, mainly hydrogen gas, and oxidizing species, principally oxygen gas and H_2O_2. The hydrogen can diffuse away from its site of formation and ferrous iron in solution can react effectively with the oxidizing species producing relatively insoluble ferric iron. The result is to transform a reducing environment into an oxidizing one. In such an oxidizing environment, some elements of concern to the nuclear waste disposal problem, particularly the actinide elements and technetium, are likely to be more soluble and less readily adsorbed than in a reducing one. The effect of radioloysis, thus, would be to render certain waste elements more mobile than they might have been in the ambient reducing environment of the host rock. These mobile elements would move through the oxidized rock until they encounter a reducing environment, i.e. rocks in which the available ferrous iron has not been oxidized by radiolysis. These mobile species would then form aureoles around the radioactive materials along an oxidation-reduction front defined by the valence state of iron.

To further develop these ideas, Christensen and Bjergbakke (31, 32) attempted to quantify the electrochemical effects of radiolysis by various types of spent fuel and high level radioactive wastes from the Swedish Nuclear Fuel Safety Project. Their considerations included various doses and dose rates of alpha, beta, gamma and

neutron radiation, the rate of hydrogen diffusion and the consequences of ferrous iron in solution.

The rocks in and around the Oklo nuclear reactors have been exposed to higher levels of radiation than any other rocks in the earth. We have examined them to see how they manifest the effects of high levels of radiation and how these effects compare with those proposed by Neretnieks (30) and Christensen and Bjergbakke (31, 32).

6.2 Iron

Ratios of Fe^{+3}/Fe^{+2} versus Al/Fe^{+2} for samples from reactor zone 2 and its aureole are plotted in Figure 2 to determine whether there have been changes in the valence state of iron. Also included in the diagram are points representing major lithologic types in the Oklo mine (19). Lines drawn from these points were calculated to show the effects of in-situ reduction of iron and addition of ferrous iron assuming that aluminum was neither added nor removed. The vast majority of the reactor zone data lie within a region on the diagram that is bounded by Fe^{+3}/Fe^{+2} in normal rock, and lines for the in-situ reduction within fine-grained pelitic sandstone and the addition of ferrous iron to sandstone or conglomerate.

Correlated changes in the ratios as shown by the lines on the diagram illustrate that it is possible to distinguish between in-situ electrochemical changes in iron and electrochemical changes associated with a net change in the abundance of iron. However, in practice these distinctions are difficult to make because they are

so dependent upon the composition of the original material. The data seem to cluster around the line representing a net gain of ferrous iron in fine-grained pelitic sandstone, the host rock of reactor zone 2.

Contrary to the suggestion of Neretnieks (30) iron in rocks that have had large radiation doses is preferentially reduced compared to that in the surrounding rocks. In fact, there is a rough correlation between the extent of radiation and the degree of iron reduction. Chemical type 1 rocks (i.e. those unambiguously associated with the nuclear reactions) show the most dramatic shift in the valence state of iron. Some contain iron that is virtually all in the reduced form. Iron in chemical types 3 and 4 (rocks from the aureoles) shows less extreme shifts in its valence state.

A shift in the electrochemical state of iron can be produced by the addition of hydrogen or the removal of oxygen. Removal of oxygen at Oklo is not a physically viable process because the oxygen fugacity was too low for such a large change to be reasonably implemented. The formation of a new mineral assemblage might shift the buffering capacity to one involving lower oxygen fugacities. This seems unlikely since the mineralogy of the reactor zones consists largely of high-temperature polymorphs of minerals found in "normal" C-1 rocks. In general, high-temperature mineral assemblages represent systems in equilibrium with higher oxygen fugacities rather than lower ones.

The most plausible explanation for the preferential reduction of

iron in the reactor zones is the addition of hydrogen produced by the radiolysis of fluids during nuclear criticality. The difference between Neretnieks' prediction (30) and our observation probably lies in the assumption of the accessibility of the radiolysis products to iron. Neretnieks' diffusion model assumes an instantaneous reaction between Fe^{+2} in the rock and the radiation-produced oxidizing agent. Our observation indicates that iron was preferentially exposed to the reducing hydrogen gas. Perhaps the accessibility of the radiolysis products to the iron, the bulk of which resides in the phyllosilicates, was determined by the relative diffusion rates in these silicate lattices. Hydrogen, being an extremely mobile specie, preferentially diffused into the solid phases producing the observed electrochemical changes.

It should be noted that the ambient fugacity of oxygen in such a system (i.e. excluding that produced by radiation) cannot be inferred from the shift in the valence state of iron. In a system which is buffered with respect to oxygen, an excess of hydrogen will only shift the relative abundances of minerals in the assemblage. The oxygen fugacity will remain fixed as long as each of the solid phases remains in the system. If the system is unbuffered, an excess of hydrogen will lower the oxygen fugacity and a shift in the relative abundances of ferrous and ferric iron will reflect this change. A shift in the oxygen fugacity cannot be inferred from changes in the relative abundances of the valence states of iron without a detailed knowledge of the phase relationships of the mineral assemblage.

6.3 The Radiation Yield of Hydrogen

Assuming that the reduction of iron was accomplished by radiation produced hydrogen, we can estimate the radiation yield of the gas, G (H_2). We must first distinguish between iron reduced by hydrogen and that which was indigenous to the rocks prior to the nuclear reactions. We consider that the relative abundances of the two iron valence states prior to the addition of hydrogen was like that presently found in the "normal" rocks of C-1, $(Fe^{+2}/Fe^{+3})_I = 1.1$. The maximum amount of iron that could have been produced by hydrogen reduction is the quantity calculated assuming the entire excess of reduced iron was transported into the rock from an external source (equation 2).

Eq 2 $$Max_{Fe_E^{+2}} = Fe_M^{+2} - Fe_M^{+3} \, (Fe^{+2}/Fe^{+3})_I$$

E signifies that ferrous iron produced by hydrogen reduction, and M the measured abundance. If the reduction was entirely in-situ, the minimum quantity of ferrous iron that could have been produced by hydrogen reduction is calculated from equation 3:

Eq 3 $$Min_{Fe_E^{+2}} = Fe_M^{+2} - Fe_T \, \frac{(Fe^{+2}/Fe^{+3})_I}{1 + (Fe^{+2}/Fe^{+3})_I}$$

Fe_T is the total measured iron in the rock. Maximum and minimum quantities of hydrogen produced ferrous iron were determined in all samples analyzed by Branche, et al. (20). These were averaged for each sample and the result is reported as excess Fe^{+2} in Table 3. For this set of samples the average rock contains 0.9% excess ferrous iron from reduction by radiolytically-produced hydrogen.

There is a clear distinction between rocks from the reactor zone and those from the aureole. The average chemical type 1 and 2 rocks contain 1.7% and 1.4% excess Fe^{+2}, respectively, while types 3 and 4 contain only 0.5%.

There is an excess of 700 mg of ferrous iron in these 77 samples from reactor zone 2 corresponding to the consumption of 4×10^{21} molecules of H_2. The samples contain 14 grams of uranium representing a total of 3×10^{26} H_2 molecules per ton of uranium. Assuming an average grain size of 500 microns, the corresponding alpha dose is 5×10^{29} eV per ton of uranium (Figure 7). Hence we calculate a $G(H_2)$ of 0.06 molecules of H_2/100 eV. If we include our estimates of beta dose this value decreases more than an order of magnitude, giving $G(H_2)$ ranging from 0.01 to 0.002 molecules H_2/100 eV. This should be considered as a lower limit since it is unlikely that all the hydrogen resulted in a reduction of iron.

6.4 Element Transport From the Reactor Zones

An important concern in the geologic storage of nuclear waste is the oxidation of certain radionuclides, thereby increasing their mobility. It is, therefore, of particular interest to examine multivalent nuclear products at Oklo to determine the effects of radiolysis on their stability. An inventory of such products in the reactor zones shows that 80% of the fission produced molybdenum, 35% of the technetium and 25% of the ruthenium are missing (13). A small fraction of the uranium has also been removed.

To transport these elements from the rocks they had to be partitioned into the mobile aqueous phase. Each of them is multivalent, forming an insoluble oxide in the reduced tetravalent state. In higher oxidation states each forms a soluble oxyanion. These dissolved species are relatively mobile in the geologic environment because of the weak adsorption of negatively charged species on immobile phases. One apparently contradictory aspect of the geochemistry of these elements at Oklo is their mobility in what is overall an extremely reduced geologic environment. We suggest that this mobility reflects oxidation by radiolytically-produced oxidizing species. This oxidation reasonably occurred on the surface of uraninite grains. It has been proposed that fission products migrated to these surfaces by solid-state diffusion (13). In addition, some portion of these elements were "injected" into the fluid phase by fission recoil from the uraninite grains. Since the mineral host and the source of radioactive emissions were one and the same, fission products at the surface of the uraninite grain were literally immersed in radiolysis products.

There is strong evidence that these elements were not redeposited within the reactor zone. No excess fission products have been observed in the reactor zone (13) and there is no indication of isotopic redistribution of uranium within the reactor zones (25). The aqueous phase within the reactor zones was sufficiently oxidizing to keep these elements in solution.

Once they were transported outside the reactor zones, these multivalent elements were redeposited. They appear to have been retained within a few meters of the reactor zones and often form aureoles comparable in size to those defined by the altered mineralogy (13, 25, 29). Once outside the reactor zones,the fluids apparently became sufficiently reducing that they could not contain their load of these dissolved fission products.

If the hydrogen that reduced iron was produced by radiolysis, then comparable quantities of another specie had to have been oxidized by the same process. If ferrous iron had been in the fluids it would have been oxidized. Hematite in fluid inclusions may reflect such an oxidation of soluble iron. However, the quantity of this iron must have been small since iron in the bulk rock is preferentially reduced. Uranium is likely to be the major specie oxidized by products of radiolysis. We have attempted to determine if the quantity of reactor zone uranium in peripheral rocks is sufficient to complement the excess of ferrous iron in the reactor zone. This assumes that uranium oxidized by the radiolysis of water was transported out of the reactor zone and deposited in the peripheral rocks. Our estimate is based on the uranium composition in the reactor zones, walls,and lateral edges as defined by Naudet (25). Portions of this data are presented in Table 6. From this data we calculate the weighted average isotopic composition of uranium in reactor zone 2 using equation 4:

Eq 4

$$\left(\frac{^{235}U}{^{235}U + ^{238}U}\right)_{Ave} = \frac{\sum_{i=1}^{10} \left({}^{235}U / \{{}^{235}U + {}^{238}U\} \right)_{M_i} \times U_{M_i}}{\sum_{i=1}^{10} U_{M_i}}$$

The subscript M refers to measured quantities.

The average 235-uranium isotopic abundance thus calculated is 0.542 atom %. We assume that uranium in the walls and lateral edges is a mixture of uranium from the core with this average isotopic composition and normal uranium (^{235}U = 0.720 atom %). The relative abundances of the two components can be calculated from equation 5.

Eq 5

$$\left(\frac{U_{RZ}}{U_N}\right) = \frac{\left(\frac{^{235}U}{^{235}U + ^{238}U}\right)_N - \left(\frac{^{235}U}{^{235}U + ^{238}U}\right)_M}{\left(\frac{^{235}U}{^{235}U + ^{238}U}\right)_M - \left(\frac{^{235}U}{^{235}U + ^{238}U}\right)_{RZ}}$$

The subscript N refers to normal uranium, M to the measured isotopic ratios, and RZ to the average isotopic composition determined for uranium in the reactor zone. Using this calculated ratio, the abundance of reactor zone uranium in the rock can be determined from equation 6.

Eq 6

$$U_{RZ}\ (g/g\ rock) = \frac{1}{1 + (U_N/U_{RZ})}\ U_{Total}$$

The average abundance of reactor zone uranium in the wall rocks is 3×10^{-2} g/g rock and 5×10^{-2} g/g rock in the uranium-rich lateral edges. To estimate how much uranium was transported from

the reactor zones we have characterized the geometry of the reactor zone based on the field observations as a cylinder 50 centimeters thick with a diameter of 20 meters. The surroundings containing the mobilized uranium is characterized as a cylinder, also based on field observations, with a thickness of one meter and a diameter of 22 meters. The cylinder of altered rock encloses the smaller cylinder of the reactor zone. The volume of altered material is thus estimated to be 220 cubic meters. Assuming the rock has a density of 2.5 g/cm^3, the total mass of altered rock is 550 tons, and the quantity of uranium transported out of the reactor zones (assuming 4×10^{-2} g U_{RZ}/g rock) is 2×10^7 grams. It is estimated that about 200 tons of uranium were involved in the nuclear reaction in zone 2 (33). Thus we estimate about 10^5 grams of uranium were removed per ton of uranium fuel corresponding to the oxidation of 2.5×10^{26} atoms of uranium per ton of uranium in the reactor zone. This quantity satisfactorily complements the 5.4×10^{26} atoms of iron reduced per ton of uranium. The calculation of quantities of oxidized uranium is very dependent on the geometry of the reactor zone and its aureoles, but we think the approximations that we used are reasonable.

If uranium was electrochemically reduced and retained within the aureoles, some element had to have been oxidized in equivalent quantity. Again the most likely candidate is iron, and thus one might expect a correlation between Fe^{+3}/Fe^{+2} and the abundance of U_{RZ} in peripheral rocks. Unfortunately,there are few such samples with data regarding both Fe^{+3}/Fe^{+2} and uranium isotopic

abundance. The thirteen samples of type 3 and 4 rocks for which such data exist seem to support such a hypothesis. Two of them (435 and 437) with significant abundances of U_{RZ} contain excess ferric iron (negative excess ferrous iron). In contrast five of these peripheral rocks with virtually no U_{RZ} (439, 441-444) contain large excesses of ferrous iron (see Tables 3 and 4). Figure 2 shows that chemical type 3 and 4 rocks generally contain larger proportions of ferric iron than rocks from the main body of the reactor zone. Indeed many of the peripheral rocks contain proportionately more oxidized iron than "normal" rocks of C-1. These trends may reflect the reduction of mobilized reactor zone uranium and a corresponding oxidation of ferrous iron.

7. COMPARISON WITH THE SWEDISH NUCLEAR FUEL SAFETY PROJECT

It is predicted that 10^{30} eV/ton of alpha radiation will be released in 10^6 years by wastes from the Swedish nuclear power program (32). This value is similar to the one we calculated for the Oklo reactors over a similar period of time. However, the beta radiation doses are markedly dissimilar in the two cases because of the enormous beta flux associated with the period of nuclear criticality at Oklo. We estimate the energy released by beta decay in the natural reactors to be 5 to 25 times that produced by alpha decay. In the Swedish wastes the energy from beta decay is predicted to be ½ to ¼ of that from alpha decay.

Despite the differences in the proportions of the two types of decay, the calculated radiation yield of hydrogen for the proposed Swedish wastes and that determined at Oklo are quite similar. Christensen and Bjergbakke (32) calculated $G(H_2)$ of 0.013 for storage of PWR fuel for a period of 10^5 years, assuming the fuel pellets to be surrounded by a thin film of water initially containing a few ppm of ferrous iron. Under similar conditions at Oklo, except for the proportion of alpha and beta decay, we have determined that the radiation yield of hydrogen was between 10^{-2} and 10^{-3} molecules/100 eV. Unless their calculations are sensitive to the proportion of radiation types, the observations regarding radiolysis at Oklo substantiate the model calculations of Christensen and Bjergbakke (32).

Under these radiation produced conditions, we observe significant deficiencies of multivalent fission products and uranium. These elements were transported no more than a few meters where they were deposited in the rocks surrounding the zones of sustained fission. We believe that the transport of these elements was induced by radiolysis produced changes in the electrochemical conditions in the rocks. Retention of the mobilized elements in peripheral rocks probably reflects the extent of the radiolysis effects and a return to ambient electrochemical conditions.

Acknowledgements: We are grateful to Ivars Neretnieks and Fred Karlsson for their interest in the Oklo natural reactors. Our appreciation to Pat Johnson and Nancy Murphy for their assistance in the preparation of the manuscript.

REFERENCES

1. Bodu, R., Bouziques, H., Marin, N., Pfiffelmann, J.-P. (1972). Geochimie nucléaire, sur l'existence d'anomalie isotopiques rencontrees dans l'uranium du Gabon. C.R. Acad. Sci., Paris, Ser. D. 275, p. 1731.

2. Weber, F. (1973). Genesis of Precambrian iron and manganese deposits. Proc. Kiev Symp. (Earth Sciences, 9), pp. 307-322.

3. Gauthier-Lafaye, F., Besnus, Y., Weber, F. (1978). Données nouvelles sur l'environment géologique des réacteur naturels. Les Reacteurs De Fission Naturels. Vienna, International Atomic Energy Agency, pp. 35-73.

4. Bonhomme, M.G., Gauthier-Lafaye, F., Weber, F. (1982). An example of lower Proterozoic sediments: the Francevillian in Gabon. Precambrian Research 18, pp. 87-102.

5. Weber, F., Geffroy, J., LeMercier, Marcelle (1975). Synthèse des études minéralogiques et pétrographiques des minerais d'Oklo, de leurs gangues et des roches encaissantes. Le Phenomene D'Oklo. Vienna, International Atomic Energy Agency, pp. 173-194.

6. Vandenbroucke, Mireille, Rouzand, J.N., Oberlin, Agnes (1978). Etude petrographique de la matiere organique d'Oklo. Les Reacteurs De Fission Naturels. Vienna, International Atomic Energy Agency, pp. 307-332.

7. Geffroy, J. (1975). Etude microscopique des minerais uranifères d'Oklo. Le Phenomene D'Oklo. Vienna, International Atomic Energy Agency, pp. 133-149.

8. Devillers, C., Ruffenach, J.-C., Menes, J., Lucas, Monique, Hagemann, R., Nief, G. (1975). Age de la minéralisation de l'uranium et date de la réaction nucléaire. Le Phenomene d'Oklo. Vienna, International Atomic Energy Agency, pp. 293-302.

9. Devillers, C. and Menes, J. (1978). Contribution du plumb et du thorium à l'histoire des réacteurs d'Oklo. Les Reacteurs De Fission Naturels. Vienna, International Atomic Energy Agency, pp. 495-511.

10. Gancarz, A.J. (1978). U-Pb age (2.05×10^9 years) of the Oklo uranium deposit. Natural Fission Reactors. Vienna, International Atomic Energy Agency, pp. 513-520.

11. Cowan, G.A., Bryant, E.A., Daniels, W.R., Maeck, W.J. (1975). Some United States studies of the Oklo phenomenon. The Oklo Phenomenon. Vienna, International Atomic Energy Agency, pp. 341-356.

12. Ruffenach, J.-C. (1978). Les réacteurs naturels d'Oklo. Etude des migrations de l'uranium et des terres rares sur une carotte de sondage et application à la détermination de la date des réactions nucléaires. Les Reacteurs De Fission Naturels. Vienna, International Atomic Energy Agency, pp. 441-471.

13. Curtis, D.B., Benjamin, T.M., Gancarz, A.J. (1983). The Oklo Reactors: Natural Analogs to Nuclear Waste Repositories. The Science and Technology of Nuclear Waste Management I. Battelle Memorial Institute, Columbus, Ohio. In Press.

14. Weber, F. (1978). Eléments pour une synthèse des resultats obtenus dans le domaine de la géologie sur les réacteurs naturels d'Oklo et leur environment. Les Reacteurs De Fission Naturels. Vienna, International Atomic Energy Agency, pp. 623-642.

15. Vidale, Rosemary J. (1978). The highest temperatures recorded by the Oklo mineral phase assemblages and rock textures. Natural Fission Reactors. Vienna, International Atomic Energy Agency, pp. 240-242.

16. Holliger, P., Devillers, C., Retali, G. (1978). Evaluation des températures neutroniques dans les zones de réaction d'Oklo par l'étude des rapports isotopiques $^{176}Lu/^{175}Lu$ et $^{156}Gd/^{155}Gd$. Ibid., pp. 553-568.

17. Openshaw, R., Pagel, M., Poty, B. (1978). Phases fluides contemporaines de la diagenèse des grès, des mouvements tectoniques et du fonctionnement des réacteurs nucléaires d'Oklo (Gabon). Ibid., pp. 267-296.

18. Dran, J.C., Durand, J.P., Langevin, Y., Maurette, M., Petit, J.C. (1978). Contribution of radiation damage studies to the understanding of the Oklo Phenomena. Ibid., pp. 375-390.

19. Gauthier-Lafaye, F. and Weber, F. (1978). Etudes minéralogiques et pétrographiques effectuées à Strasbourg sur les réacteurs naturels d'Oklo. Ibid., pp. 199-227.

20. Branche, F., Chantret, F., Guillemant, A., Pouget, R. (1975). Données chimiques et minéralogiques sur le gisement d'Oklo. Le Phenomene D'Oklo. Vienna, International Atomic Energy Agency, pp. 119-132.

21. Simpson, P.R. and Bowles, J.F.W. (1978). Mineralogical evidence for the mode of deposition and metamorphism of reaction zone samples from Oklo. Les Reacteur De Fission Naturels. Vienna, International Atomic Energy Agency, pp. 297-306.

22. Havette, Andrée, Naudet, R., Slodzian, G. (1975). Etude par analyse ionique de la répartition et des proportions isotopiques de certains éléments dans les échantillons d'Oklo. Le Phenomene d'Oklo. Vienna, International Atomic Energy Agency, pp. 463-477.

23. Naudet, R. (1978). Etude paramétrique de la criticité des réacteurs naturels. Les Reacteurs De Fission Naturels. Vienna, International Atomic Energy Agency, pp. 589-600.

24. Maeck, W.J., Spraktes, F.W., Tromp, R.L., Keller, J.H. (1975). Analytical results, recommended nuclear constants and suggested correlations for the evaluation of Oklo fission-product data. The Oklo Phenomenon. Vienna, International Atomic Energy Agency, pp. 319-340.

25. Naudet, R. (1978). Synthèse des données concernant la stabilité et les remobilisations de l'uranium et des terres rares. Les Reacteurs De Fission Naturels. Vienna, International Atomic Energy Agency, pp. 643-676.

26. Duffy, C.J. (1978). Uranium solubilities in the Oklo reactor zones. Ibid., pp. 225-232.

27. Gancarz, A.J., Cowan, G.A., Curtis, D., Maeck, W. (1980). ^{99}Tc, Pb and Ru migration around the Oklo natural fission reactors. Scientific Basis for Nuclear Waste Management, 2. New York, Plenum Press, pp. 601-608.

28. Bryant, E.A., Cowan, G.A., Daniels, W.R., Maeck, W.J. (1976). Oklo, an experiment in long-term geologic storage. Actinides in the Environment. American Chemical Society, pp. 89-102.

29. Curtis, D.B., Benjamin, T.M., Gancarz, A.J., Delmore, J. (1982). Geochemistry of Technetium Studies of the Oklo Reactors. Proceedings of the 5th International Conference on Geochronology, Cosmochronology and Isotope Geology. Nikko, Japan, July 1982.

30. Neretnieks, Ivars (1982). The movement of a redox front from a repository for nuclear waste. Personal Communication.

31. Christensen, Hilbert and Bjergbakke, Erling (1982). Radiolysis of groundwater from HLW stored in copper canisters. KBS Technical Report 82-02.

32. Christensen, Hilbert and Bjergbakke, Erling (1983). Radiolysis of ground water from spent fuel. Studsvik/NW-82/364. In preparation.

33. Naudet, R. (1978). Les réacteurs d'Oklo, cinq ans d'exploration du site. Les Reacteurs De Fission Naturels. Vienna, International Atomic Energy Agency, pp. 3-18.

Table 1 Organic Carbon in Rocks from the Oklo Mine*

Lithologic Type	Distance From Reactor Zones (m)	Uranium Abundance (wt. %)	Organic Carbon (wt. %)
Argillite	Core	Rich	0.04
Argillite	Core	Rich	0.05
Argillite	Core	6	0.14
Argillite	Core	18	0.20
Argillite	Core	36	0.02
Argillite	Border	Rich	0.12
Argillite	Border	Rich	0.05
Argillite	Border	32	0.41
Sandstone	Border	Rich	0.11
Sandstone	0.5	20	0.13
Sandstone	0.8	Rich	0.08
?	1.	Poor	0.14
Sandstone	1.	19	0.15
Argillite	1.5	25-30	0.35
Argillite	1.6	?	1.06
Sandstone	2.	Poor	0.23
Sandstone	2.	8	0.14
Sandstone	2.	15	0.16
Argillite	3.	25-30	0.09
Sandstone	2-3	Poor	0.08
?	3.	Poor	0.16
?	4.	Poor	0.30
Sandstone	4.5	8.5	0.18
Sandstone	12.	8.3	0.85
Sandstone	?	9.3	1.53
Sandstone	500.	Poor	0.20

*Vandenbrouke, et al. (1977)

Table 2 Chemical Composition of Samples from Oklo Mine*

Sample No.	Si / Al	Ca / Al	Mg / Al	K / Al	U / Al	Chemical Type
2L Traverse of Reactor Zone 2						
395	1.2	0.03	0.94	0.02	0.15	3
396	1.3	0.05	1.0	0.03	0.14	3
397	1.3	0.05	0.52	0.09	0.64	
398	0.4	0.07	0.43	0.10	1.8	
399	2.0	0.28	0.43	0.13	11.0	1
400	1.5	0.30	0.41	0.15	16.0	1
401	1.5	0.08	0.32	0.11	3.4	
402	1.5	0.57	0.53	0.11	31.0	1
403	1.5	0.41	0.55	0.11	27.0	1
404	1.4	0.33	0.47	0.10	19.0	1
405	1.7	0.81	0.63	0.14	44.0	1
406	1.5	0.46	0.44	0.10	18.0	1
407	0.83	0.28	0.67	0.11	16.0	1
408	1.4	0.13	0.49	0.08	6.9	1
409	1.3	0.03	0.59	0.05	1.1	
410	2.1	0.10	0.53	0.11	5.4	1
411	1.4	0.11	0.55	0.07	6.2	1
412	1.5	0.10	0.57	0.09	5.7	1
413	1.4	0.03	0.61	0.06	1.2	
414	1.2	0.01	1.0	0.017	0.09	3
2N Traverse of Reactor Zone 2						
415	1.2	0.01	0.79	0.04	0.08	3
416	1.2	0.01	0.64	0.09	0.07	3
417	1.3	0.03	0.43	0.11	0.63	
418	1.3	0.05	0.23	0.18	1.6	2
419	1.2	0.06	0.20	0.18	1.6	2
420	1.2	0.06	0.16	0.18	2.8	2
421	1.4	0.03	0.11	0.27	1.3	2
422	1.3	0.03	0.12	0.26	1.0	2

Table 2 Chemical Composition of Samples from Oklo Mine (Cont'd)

Sample No.	Si/Al	Ca/Al	Mg/Al	K/Al	U/Al	Chemical Type
2N Traverse of Reactor Zone 2, cont'd						
423	1.4	0.04	0.13	0.35	1.9	2
424	1.4	0.10	0.12	0.32	2.1	2
425	1.5	0.04	0.13	0.30	1.6	2
426	1.4	0.04	0.13	0.26	1.4	2
427	1.9	0.09	0.21	0.19	5.1	1
428	1.4	0.19	0.27	0.18	12.0	1
429	1.3	0.25	0.28	0.16	13.0	1
445	1.2	0.14	0.24	0.14	7.5	1
446	1.3	0.14	0.22	0.14	7.9	1
447	1.3	0.06	0.17	0.15	3.2	2
448	1.3	0.04	0.22	0.17	1.9	2
449	1.3	0.07	0.30	0.18	3.5	2
2P Traverse of Reactor Zone 2						
430	1.4	0.19	0.39	0.13	10.0	1
431	1.3	0.27	0.40	0.13	16.0	1
432	1.5	0.15	0.41	0.15	8.8	1
433	1.5	0.20	0.46	0.14	11.0	1
434	2.9	0.05	0.23	0.24	2.7	
435	2.0	0.02	0.28	0.10	0.15	4
436	4.1	0.03	0.25	0.17	0.38	4
437	2.8	0.02	0.15	0.22	0.34	4
438	3.7	0.02	0.17	0.30	0.18	4
439	4.7	0.03	0.13	0.36	0.17	4
440	4.1	0.02	0.12	0.29	0.22	4
441	3.6	0.02	1.2	0.14	0.14	4
442	1.5	0.01	0.95	0.01	0.05	3
443	1.4	0.005	1.4	0.006	0.03	3
444	1.3	0.007	1.1	0.010	0.01	3

Table 2 Chemical Composition of Samples from Oklo Mine (Cont'd)

Sample No.	Si / Al	Ca / Al	Mg / Al	K / Al	U / Al	Chemical Type
Quarry Sample from Unknown Location						
312	41.0	0.15	0.14	0.19	0.59	
313	20.0	0.13	0.09	0.04	10.0	
314	27.0	0.14	0.11	0.10	8.4	
Sounding KN-50 Near Reactor Zone 2						
315	2.0	0.02	0.27	0.32	0.14	
316	1.7	0.01	0.27	0.31	0.001	
317	1.3	0.01	0.08	0.37	0.001	
318	1.4	0.01	0.23	0.42	0.07	
319	1.3	0.003	1.0	0.004	0.005	3
320	1.6	0.02	1.0	0.02	0.06	3
321	1.4	0.02	0.61	0.08	0.70	3
322	1.4	0.003	0.82	0.02	0.007	3
323	1.7	0.03	0.33	0.20	0.64	
324	1.5	0.02	0.95	0.03	0.10	3
325	1.3	0.003	1.2	0.009	0.002	3
326	1.2	0.02	1.2	0.004	0.002	3
327	1.3	0.006	1.1	0.002	0.0007	3
Sounding KN-47 Near Reactor Zone 1						
328	340.0	1.4	1.1	1.1	3.7	
329	14.0	0.36	0.30	0.18	0.05	
330	1.7	0.01	0.04	0.46	0.12	
331	14.0	0.04	0.08	0.25	0.02	
332	1.4	0.02	0.07	0.31	0.27	
333	4.9	0.02	0.14	0.34	0.002	
Type 1	<2	>0.1	>0.4	>0.1	>5	
Type 2	<2	<0.1	0.4>0.1	>0.1	5>1	
Type 3	<2	<0.1	>0.7	<0.1	<1	
Type 4	>2	<0.1	<0.3	>0.1	<1	

*Branche, et al. (1975)

Table 3 Properties of Iron in Samples from Oklo Mine*

Sample No.	$\frac{Fe^{+3}}{Fe^{+2}}$	$\frac{Al}{Fe^{+2}}$	Fe Total (wt. %)	Excess Fe^{+2} (wt. %)	Chemical Type
2L Traverse of Reactor Zone 2					
395	0.87	2.3	8.7	0.12	3
396	0.84	2.1	9.1	0.23	3
397	0.83	3.2	6.4	0.23	
398	0.44	2.1	6.6	1.8	
399	0.02	1.0	3.9	2.7	1
400	0.10	1.1	3.3	1.9	
401	1.3	2.4	7.3	-1.0	1
402	0.64	1.2	2.6	0.34	1
403	0.08	0.85	2.9	1.8	1
404	0.15	0.99	3.4	1.8	1
405	0.63	1.1	2.1	0.29	1
406	0.15	1.1	3.4	1.8	1
407	0.09	0.96	3.8	2.3	1
408	0.09	1.2	5.0	3.0	1
409	0.55	2.3	6.7	1.2	
410	0.13	1.5	4.3	2.4	1
411	0.65	2.2	4.5	0.58	1
412	0.56	2.2	4.5	0.82	1
413	0.37	2.1	6.6	2.1	
414	0.67	3.5	5.5	0.62	3
2N Traverse of Reactor Zone 2					
415	0.74	2.8	7.5	0.56	3
416	1.1	3.7	6.8	-0.40	3
417	0.93	3.4	6.6	-0.09	
418	0.21	2.6	4.9	2.3	2
419	0.26	2.4	5.3	2.2	2
420	0.50	3.0	4.6	1.0	2
421	0.55	3.9	4.3	0.81	2
422	1.3	5.7	4.5	-0.58	2
423	0.37	3.2	3.9	1.2	2
424	0.13	2.8	4.0	2.2	2

Table 3 Properties of Iron in Samples from Oklo Mine (Cont'd)

Sample No.	$\frac{Fe^{+3}}{Fe^{+2}}$	$\frac{Al}{Fe^{+2}}$	Fe Total (wt. %)	Excess Fe^{+2} (wt. %)	Chemical Type
2N Traverse of Reactor Zone 2 (cont'd)					
425	0.12	3.2	3.8	2.1	2
426	1.0	5.0	4.6	-0.26	2
427	0.90	2.8	4.7	0	1
428	0.20	1.4	3.8	1.8	1
429	0.34	1.6	3.2	1.1	1
445	0.19	2.8	4.4	2.1	1
446	0.46	2.2	3.8	0.93	1
447	0.17	1.9	5.5	2.8	2
448	0.27	2.7	5.0	2.4	2
449	0.18	2.1	4.7	2.3	2
2P Traverse of Reactor Zone 2					
430	0.11	0.71	6.4	3.7	1
431	0.25	0.83	4.8	2.0	1
432	0.52	1.1	6.6	1.3	1
433	0.23	0.77	6.1	2.7	1
434	0.40	2.5	3.9	1.1	
435	1.0	4.0	5.6	-0.31	4
436	0.81	3.2	3.8	0.16	4
437	1.3	4.3	4.6	-0.69	4
438	0.64	5.4	2.5	0.33	4
439	0.15	2.2	3.5	1.9	4
440	0.89	5.7	2.5	0.01	4
441	0.22	1.9	4.4	2.1	4
442	0.39	2.4	6.8	2.0	3
443	0.48	2.3	6.7	1.6	3
444	0.53	3.0	6.1	1.2	3
Quarry Samples from Unknown Location					
312	0.88	1.7	1.2	0.01	
313	0.11	0.83	2.1	1.2	
314	0.07	0.56	2.4	1.5	

Table 3 Properties of Iron in Samples from Oklo Mine (Cont'd)

Sample No.	$\frac{Fe^{+3}}{Fe^{+2}}$	$\frac{Al}{Fe^{+2}}$	Fe Total (wt. %)	Excess Fe^{+2} (wt. %)	Chemical Type
Sounding KN-50 Near Reactor Zone 2					
315	0.94	6.6	3.5	-0.05	
316	1.2	9.3	3.1	-0.36	
317	0.34	8.3	2.6	0.92	
318	2.6	26.	1.9	-0.73	
319	0.61	2.9	6.4	0.95	3
320	1.2	2.6	8.4	-0.82	3
321	1.2	3.5	6.8	-0.86	3
322	0.82	3.9	5.7	0.23	3
323	1.4	4.3	5.8	-0.92	
324	1.6	3.6	7.4	-1.6	3
325	0.7	3.4	5.6	0.58	3
326	0.7	3.1	6.3	0.61	3
327	0.6	2.9	6.4	0.98	3
Sounding KN-47 Near Reactor Zone 1					
328	0.65	0.65	0.32	0.04	
329	0.47	1.6	2.6	0.62	
330	2.5	29.	1.7	-0.62	
331	27.	34.	2.4	-1.3	
332	1.6	14.	2.5	-0.53	
333	0.52	3.1	3.4	0.71	

*Branche, et al. (1975)

Table 4 Uranium Properties in Samples from Oklo Mine

Sample No.	UO_2* (wt. %)	^{235}U** (atomic %)	Excess U_{RZ} (wt. %)	Chemical Type
2L Traverse of Reactor Zone 2				
395	1.8	0.698	0.20	3
396	1.6	0.677	0.34	3
397	8.1	0.61		
398	19.2	0.53		
399	48.9	0.57		1
400	63.7	0.45		1
401	29.7	0.41		
402	68.6	0.56		1
403	69.9	0.5724		1
404	63.9	0.5541		1
405	69.7	0.5575		1
406	63.6	0.5576		1
407	61.7	0.5113		1
408	43.5	0.5165		1
409	12.1	0.60		
410	36.1	0.5759		1
411	42.1	0.5913		1
412	40.7	0.6031		1
413	13.3	0.630		
414	1.2	0.658	0.37	3
2N Traverse of Reactor Zone 2				
415	1.1			3
416	1.0			3
417	8.2	0.7130		
418	18.5	0.707		2
419	18.8	0.700		2
420	29.2	0.677		2
421	16.3	0.7155		2
422	13.0	0.690		2
423	19.2	0.711		2

Table 4 Uranium Properties in Samples from Oklo Mine (Cont'd)

Sample No.	UO_2* (wt. %)	^{235}U** (atomic %)	Excess U_{RZ} (wt. %)	Chemical Type
2N Traverse of Reactor Zone 2 (cont'd)				
424	24.0	0.695		2
425	19.9	0.62		2
426	18.4			2
427	37.8	0.561		1
428	57.7	0.57		1
429	58.1			1
445	48.1	0.56		1
446	50.3	0.599		1
447	31.7	0.5985		2
448	23.0	0.586		2
449	32.8	0.612		2
430	47.5	0.5703		1
431	58.0	0.5431		1
432	45.2	0.42		1
433	49.2	0.43		1
434	21.3	0.40		
435	1.9	0.6993	0.20	4
436	2.9	0.6900	0.43	4
437	3.3	0.6848	0.57	4
438	1.7	0.63	0.76	4
439	1.3	0.7105	0.06	4
440	1.9	0.6810	0.37	4
441	1.1	0.7092	0.06	4
442	0.6	0.6944	0.08	3
443	0.3	0.6974	0.03	3
444	0.2	0.6921	0.03	3

*Branche, et al.(1975)

**Naudet and Renson (1975)

Table 5 Relative Abundances of Elements in Fluid From the Francevillian Basin

	K/Na	Ca/Na	Mg/Na	$SO_4^{=}/Cl^-$
Ambient Fluids				
50 meters from reactor zone	0	0.023	0	0.10
	0.091	0.061	0.009	0.028
	0.093	0.071	0.011	0.055
	0.084	0.088	0.011	0.053
	0.093	0.071	0	0.086
	0.093	0.028	0	0.12
	0.11	0.076	0.013	0.095
25 kilometers from Oklo	0.101	0.24	0.028	0.210
	0.073	0.23	0.026	0.423
	0.040	0.44	0.026	0.039
Reactor Zone Fluids				
	0.16	0.12	0.040	0.20
	0.19	0.20	0.055	0.51
	0.16	0.49	0.041	0.14
	0.21	1.1	0.12	0.73
	0.23	0.76	0.10	1.5
	0.24	1.8	0.18	0.83
	0.20	1.3	0.14	0.57

Table 6 Uranium Properties in Reactor Zones and Peripheral Rocks*

Distance From Reactor Zone 2 (m)	UO_2 (wt. %)	^{235}U (atomic %)	Excess U_{RZ} (wt. %)
Core			
0	23	0.323	
0	20	0.313	
0	10	0.348	
0	45	0.444	
0	11	0.557	
0	70	0.578	
0	19	0.615	
0	39	0.621	
0	54	0.658	
0	48	0.670	
Walls			
0.2	20	0.676	4.4
0.4	9	0.669	2.3
0.6	19	0.663	5.4
0.9	8	0.678	1.7
2.20	5	0.712	0.20
0.10	1	0.634	0.43
0.30	0.5	0.714	0.01
0.60	0.8	0.713	0.03
0.90	8	0.717	0.12
Rich Lateral Edges			
Close	54	0.690	8.0
Close	36	0.694	4.6
Close	57	0.694	7.3
Close	66	0.698	6.2
0.80	34	0.717	0.5
1.00	36	0.719	0.18
2.30	$\sim$ 28	0.720	

*Naudet (1977)

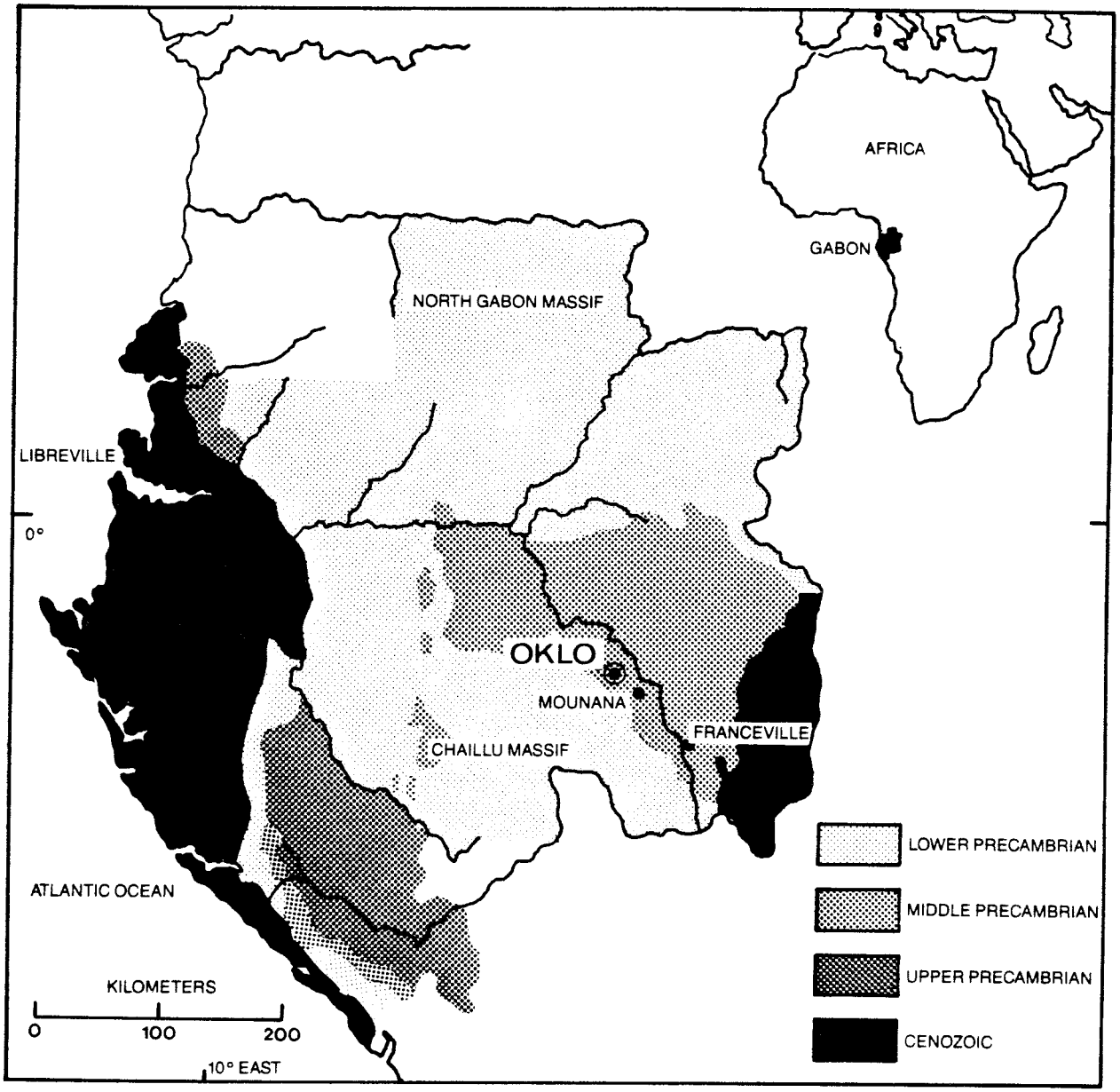

Figure 1 A map showing the location of the Oklo uranium mine in the Republic of Gabon.

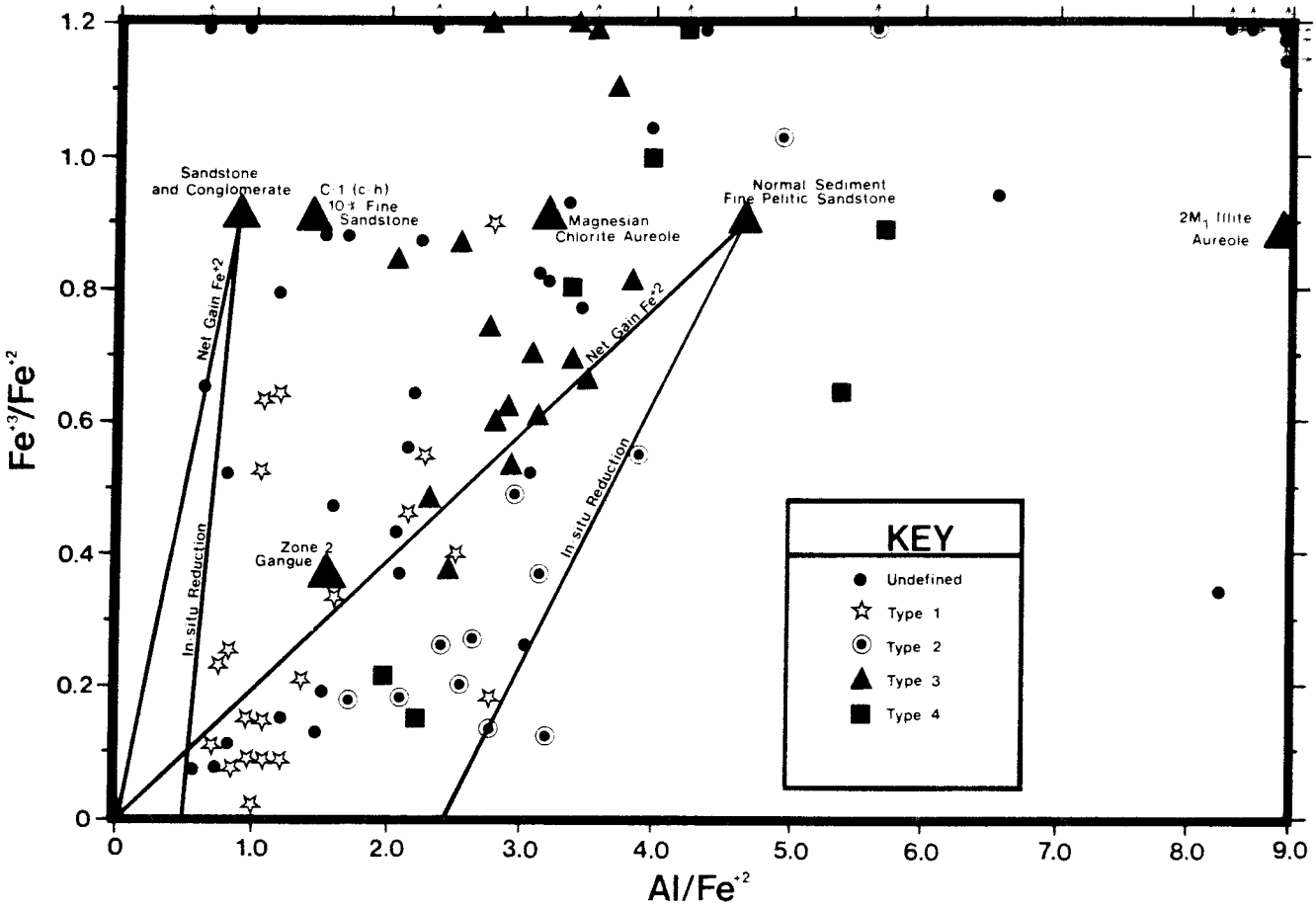

Figure 2 Plot of Fe^{+3}/Fe^{+2} vs. Al/Fe^{+2} from samples of reactor zone 2 and its aureoles. The large triangles identify these properties in principal lithologic types from C-1, the uranium mineralized stratum containing the reactor zones. Lines emanating from these points show the change in these chemical properties resulting from in-situ reduction of iron and the addition of ferrous iron to the appropriate lithologic type.

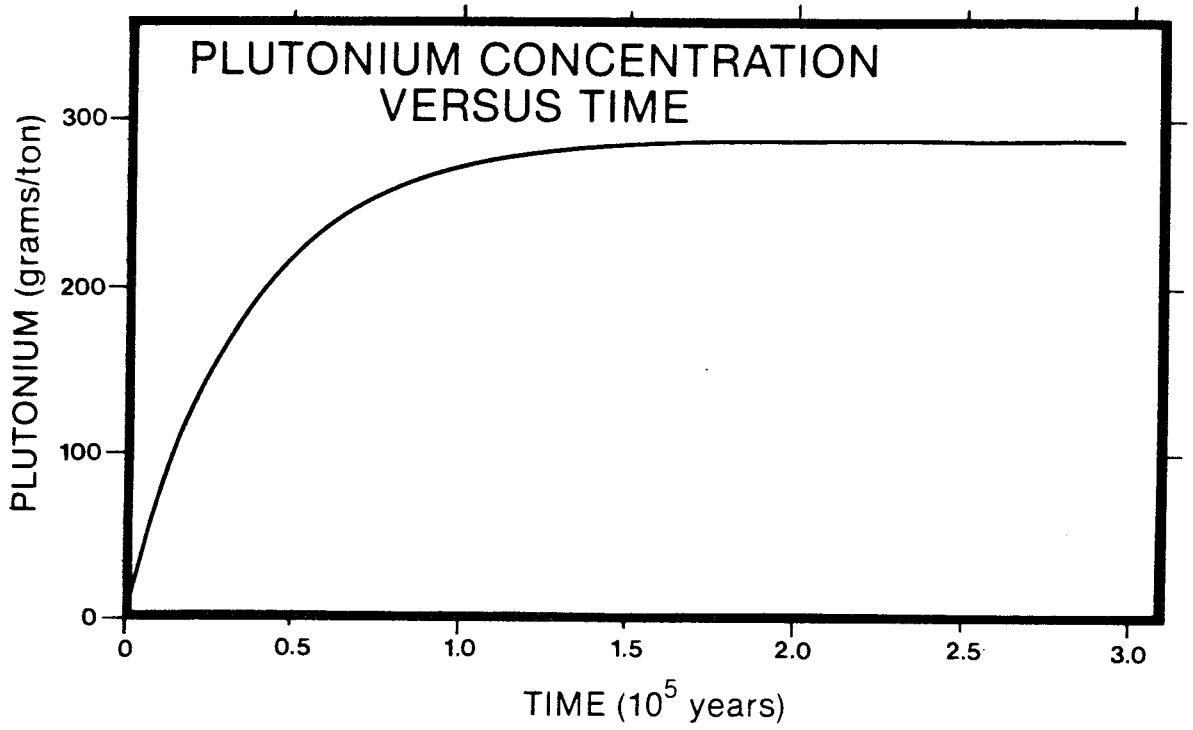

Figure 3 Abundance of 239-plutonium in the Oklo reactors as a function of time since the beginning of nuclear criticality.

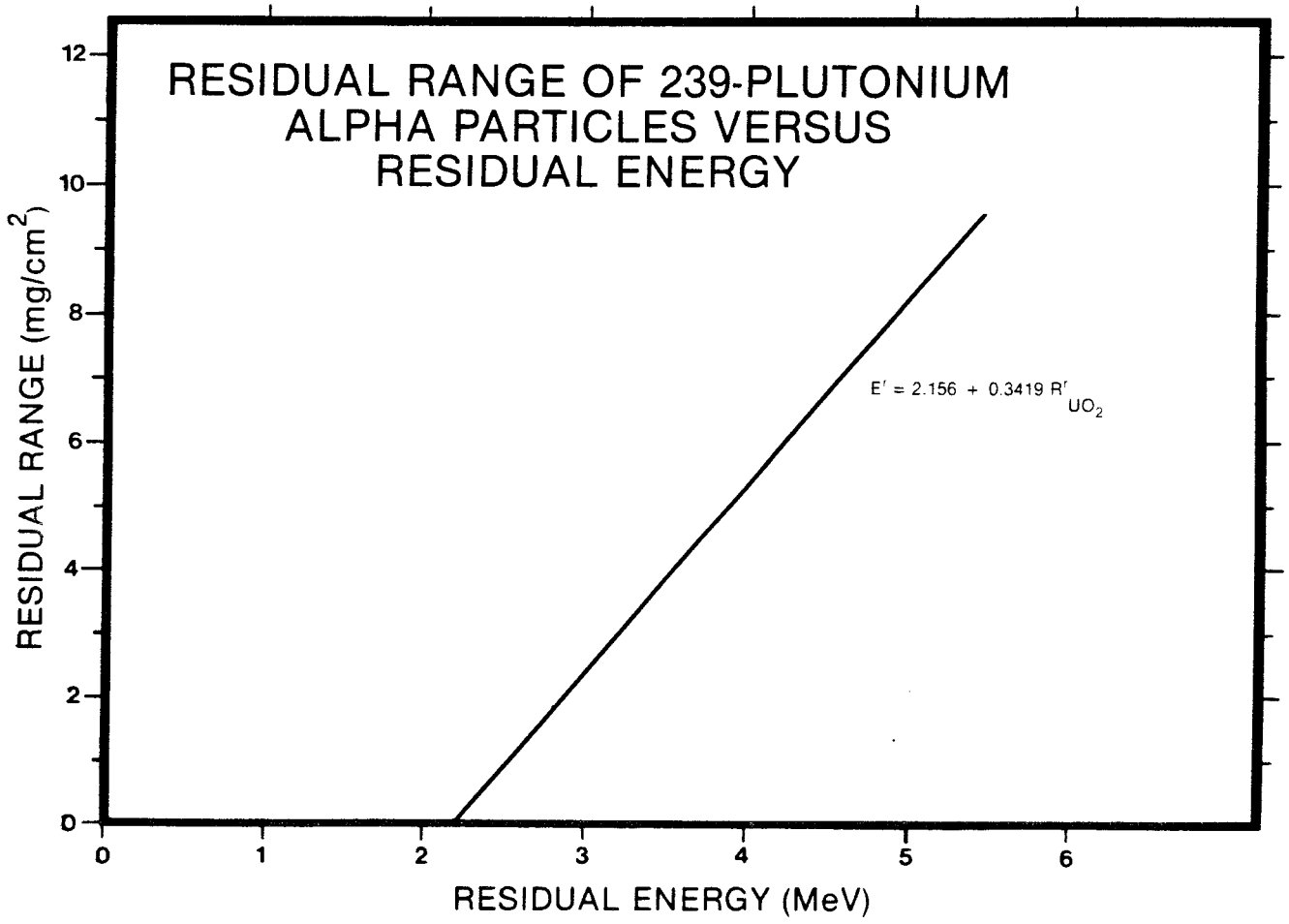

Figure 4 A plot showing the residual energy of alpha particles emitted by the decay of 239-plutonium as a function of residual range.

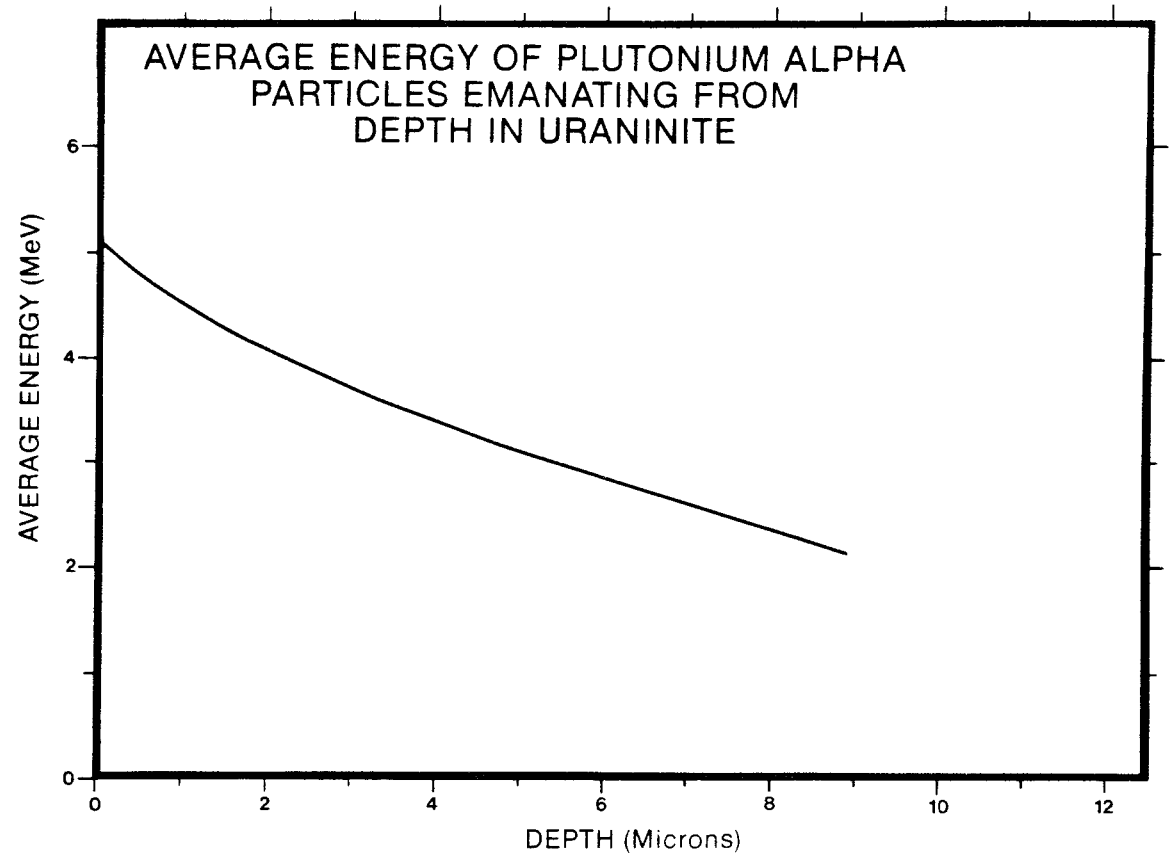

Figure 5 Average energy of alpha particles from the decay of 239-plutonium as a function of depth in uraninite.

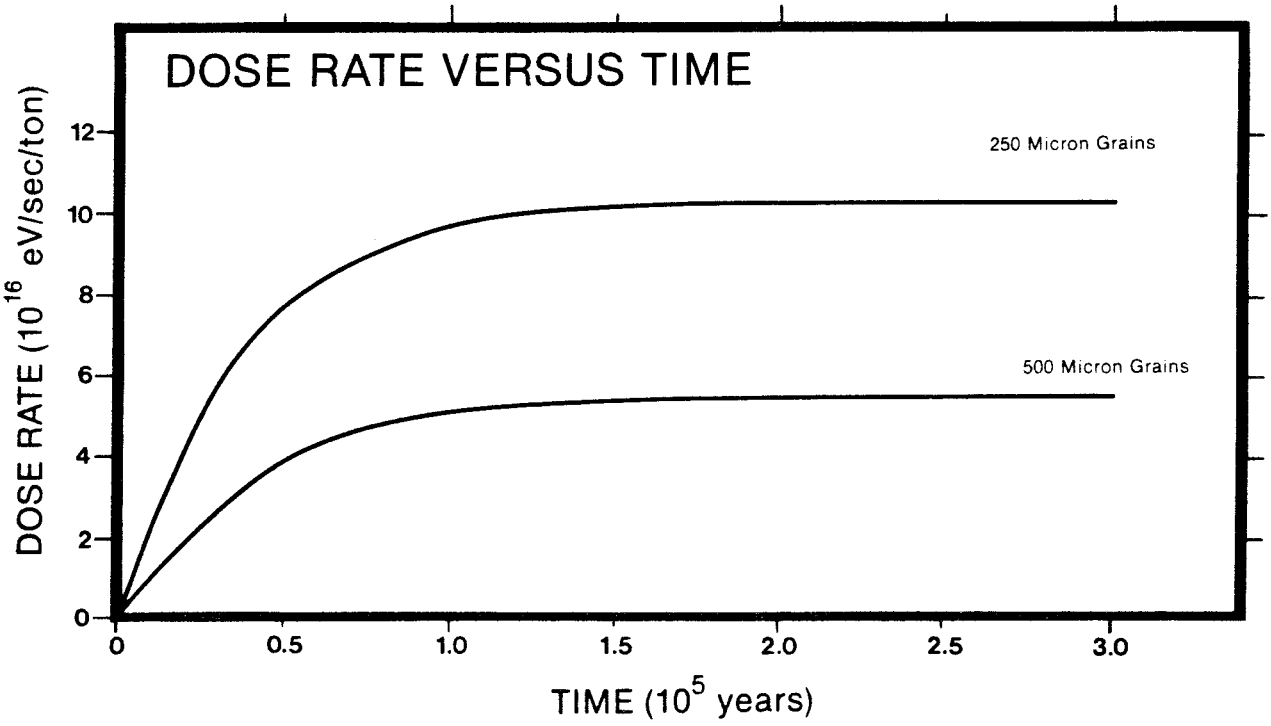

Figure 6 Dose rate from 239-plutonium alpha particles as a function of time from the beginning of nuclear criticality for different size grains of uraninite.

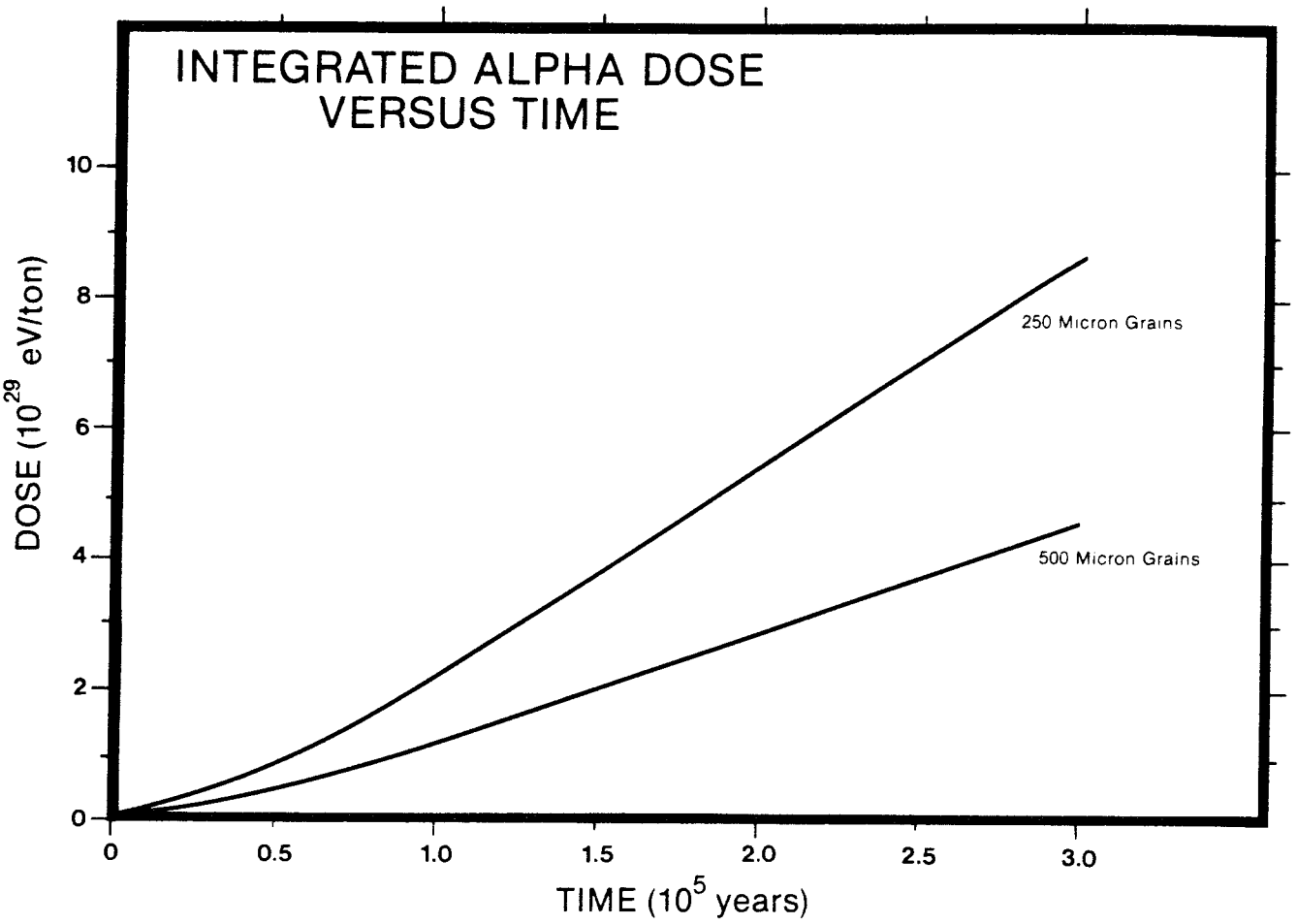

Figure 7 Total dose from 239-plutonium alpha particles as a function of time from the beginning of nuclear criticality for different size grains of uraninite.

LIST OF KBS's TECHNICAL REPORTS

1977-78

TR 121 KBS Technical Reports 1 - 120.
Summaries. Stockholm, May 1979.

1979

TR 79-28 The KBS Annual Report 1979.
KBS Technical Reports 79-01--79-27.
Summaries. Stockholm, March 1980.

1980

TR 80-26 The KBS Annual Report 1980.
KBS Technical Reports 80-01--80-25.
Summaries. Stockholm, March 1981.

1981

TR 81-17 The KBS Annual Report 1981.
KBS Technical Reports 81-01--81-16
Summaries. Stockholm, April 1982.

1983

TR 83-01 Radionuclide transport in a single fissure
A laboratory study
Trygve E Eriksen
Department of Nuclear Chemistry
The Royal Institute of Technology
Stockholm, Sweden 1983-01-19

TR 83-02 The possible effects of alfa and beta radiolysis on the matrix dissolution of spent nuclear fuel
I Grenthe
I Puigdomènech
J Bruno
Department of Inorganic Chemistry
Royal Institute of Technology
Stockholm, Sweden January 1983

TR 83-03 Smectite alteration
Proceedings of a colloquium at State University of New York at Buffalo, May 26-27, 1982
Compiled by Duwayne M Anderson
State University of New York at Buffalo
February 15, 1983

TR 83-04 Stability of bentonite gels in crystalline rock - Physical aspects
Roland Pusch
Division Soil Mechanics, University of Luleå
Luleå, Sweden, 1983-02-20

TR 83-05 Studies of pitting corrosion on archeological bronzes
Åke Bresle
Jozef Saers
Birgit Arrhenius
Archeological Research Laboratory
University of Stockholm
Stockholm, Sweden 1983-02-10

TR 83-06 Investigation of the stress corrosion cracking of pure copper
L A Benjamin
D Hardie
R N Parkins
University of Newcastle upon Tyne
Department of Metallurgy and Engineering Materials
Newcastle upon Tyne, Great Britain, April 1983

TR 83-07 Sorption of radionuclides on geologic media - A literature survey. I: Fission Products
K Andersson
B Allard
Department of Nuclear Chemistry
Chalmers University of Technology
Göteborg, Sweden 1983-01-31

TR 83-08 Formation and properties of actinide colloids
U Olofsson
B Allard
M Bengtsson
B Torstenfelt
K Andersson
Department of Nuclear Chemistry
Chalmers University of Technology
Göteborg, Sweden 1983-01-30

TR 83-09 Complexes of actinides with naturally occurring organic substances - Literature survey
U Olofsson
B Allard
Department of Nucluear Chemistry
Chalmers University of Technology
Göteborg, Sweden 1983-02-15

TR 83-10 Radiolysis in nature:
Evidence from the Oklo natural reactors
David B Curtis
Alexander J Gancarz
New Mexico, USA February 1983

TR 83-11 Description of recipient areas related to final storage of unreprocessed spent nuclear fuel

Björn Sundblad
Ulla Bergström
Studsvik Energiteknik AB
Nyköping, Sweden 1983-02-07